nature ecology & evolution

SUPPLEMENTARY INFORMATION

https://doi.org/10.1038/s41559-017-0415-0

In the format provided by the authors and unedited.

Consistent effects of biodiversity loss on multifunctionality across contrasting ecosystems

Nicolas Fanin[1,2*], Michael J. Gundale[1], Mark Farrell[3], Marcel Ciobanu[4], Jeff A. Baldock[3], Marie-Charlotte Nilsson[1], Paul Kardol[1] and David A. Wardle[1,5]

[1]Department of Forest Ecology and Management, Swedish University of Agricultural Sciences, Umeå, Sweden. [2]Institut National de la Recherche Agronomique, UMR 1391 Interaction Soil Plant Atmosphere, Bordeaux Sciences Agro, 71 Avenue Edouard Bourlaux, Villenave-d'Ornon, France. [3]CSIRO Agriculture and Food, Locked Bag 2, Glen Osmond, South Australia, Australia. [4]Institute of Biological Research, Republicii Street 48, Cluj-Napoca, Romania. [5]Asian School of the Environment, Nanyang Technological University, 50 Nanyang Avenue, Singapore. *e-mail: nicolas.fanin@inra.fr

Supplementary Information contains:

Two Supplementary Methods:

Ten Supplementary Tables:

Thirteen Supplementary Figures:

Supplementary Methods 1 | Community sequencing

Extraction and amplification. To assess the fungal community structure by high-throughput sequencing of amplified ITS2 markers, we employed the method of Ihrmark et al.[1], as modified by Clemmensen et al.[2]. For the core from each plot, DNA was extracted from freeze-dried organic matter (50 mg) using the NucleoSpin Soil Kit (Macherey-Nagel, Düren, Germany). Fungal ITS2 fragments were amplified using gITS7[1] and ITS4[3] primer combination with both primers extended with 8 bp long sample-specific tags. The 30 μL PCR reactions consisted of 0.2 mM dNTPs, 0.75 mM $MgCl_2$, 0.5 μM fITS9 primer, 0.3 μM ITS4 primer and 0.75 U DNA polymerase (DreamTaq Green; Thermo Fisher Scientific, Waltham, MA, USA). PCR cycling conditions were 95 s at 94°C and 20–35 cycles of 30 s at 94°C, 30 s at 56°C, 30 s at 72°C and a final 7 min at 72°C. Template concentrations and number of PCR cycles were optimized for each sample (based on preliminary qPCR assays), aiming PCR reactions to be interrupted in the exponential phase, during which amplification is more quantitatively accurate. Each sample was run in triplicate to reduce stochastic PCR distortion of community composition. Negative controls (for DNA extraction and PCR) were also used to check potential contamination and product quality in each series. Amplicons were then purified using the Agencourt AMPure kit (Beckman Coulter, Beverly, MA, USA) and concentrations were measured fluorometrically (Qubit Fluorometer, Invitrogen, Carlsbad, CA, USA). Equal amounts of PCR product from each sample were pooled into five composite samples for sequencing. Adaptor ligation and PacBio (PSII) sequencing of amplicons were conducted by SciLifeLab, Uppsala, Sweden.

Bioinformatics. Sequences were processed using the bioinformatics pipeline SCATA (http://scata.mykopat.slu.se/). Sequences with an average quality score below 20 or below 3 at any

single position were discarded. Sequences with missing primer sequences or missing or mismatching identification tags were also discarded. Out of the total of 1596891 sequences, 617658 sequences passed this first quality control (median length of 266 bases). Sequences with missing primer sequences or identification tags were also discarded. During the SCATA clustering procedure, sequences were compared for similarity using USEARCH as a search engine, with the minimum length of pairwise alignments set to 60% of the longest sequence. Pairwise alignments were scored using a scoring function with 1 in penalty for mismatch, 0 for gap opening and 1 for gap extension. Homopolymers were collapsed to 3 bp before alignment. Sequences were clustered into operational taxonomic units (OTUs) by single linkage clustering with a 98.5% sequence similarity required to enter OTUs. Global singletons were deleted. For the whole study, 601968 high quality sequences (on average 1436 per sample, ranging between 50 and 4761) were assembled into 3008 global, species-level OTUs. For establishment of relative abundance of fungal sequence clusters, all non-fungal sequence reads (on average 13.6% of the sequences obtained) were removed from the data. To cover at least 85% of the fungal reads in each sample type (95.4% of all reads identified on average), representative sequences of the globally most abundant 514 fungal OTUs, each represented by at least 50 sequences, were identified and when possible assigned to functional guilds by comparison to UNITE Envir and annotated INSD reference data bases using the massBLASTer option in the UNITE phylogenetic module (https://unite.ut.ee/)[4]. For each identification, we considered the 10 best-matching references to annotate our global sequences as accurately as possible. If no reliable taxon name was available, we ran manual BLASTn searches against INSDC with 500 best matching sequences as output. In line with Terdersoo et al.[5], we typically relied on 98.0%, 90.0%, 85.0%, 80.0%, and 75.0% similarity as a criterion for assigning names of a species, genus, family, order, or class, respectively, except for Sordariomycetes, Leotiomycetes, and Eurotiomycetes for which the similarity levels have been

raised because these taxa contain multiple genera and families that have unusually conserved ITS sequences. As proposed by the same authors, we considered values of BLASTn search results $<e^{-50}$ reliable to assign sequences to the fungal kingdom, whereas those $>e^{-20}$ were considered 'unknown'. E-values between e^{-20} and e^{-50} were manually checked against the 10 best hits for accurate assignment. The identification work was done twice independently, to certify objectivity when assigning a name to each fungal OTU.

Functional group assignation. We then employed a phylogenetically and taxonomically flexible delimitation level of functional groups guided by external reference sequences downloaded from public databases. Fungi identified to species or genera with a well-known function or life-form (i.e., based on published literature) were categorized into functional groups: 'Litter-associated saprotrophs', 'Molds and yeasts', 'Pathogens and parasites', 'Lichens', 'Ectomycorrhizal fungi', 'Ericoid mycorrhizal fungi' or 'Root-associated fungi'. This last category included species matching reference sequences isolated from roots or rhizoids (other than ericoid or ectomycorrhizal) as well as fungi with uncertain mycorrhizal type. Fungi included in supported clades representing either a higher phylogenetic level with common function (i.e., Archaeorhizomycetes), or derived from a particular substrate (i.e., surface-sterilized roots of ectomycorrhizal- or ericoid hosts or litter) were categorized into putative functional groups: 'Putative litter-associated saprotrophs', 'Putative ectomycorrhizal fungi', 'Putative ericoid mycorrhizal fungi' or 'Putative root-associated fungi'. If different functional categories were present within a specific species, we chose the dominant group (>75% of species assigned to a specific category) or considered its ecology unknown (<75% of species assignable to a single category). Clusters of low abundance or with insufficient information for being classified in a putative functional group were left in the group of 'Fungi with unknown function'.

Supplementary Methods 2 | Field and laboratory measurements

Plant biomass. In the field, we estimated aboveground dwarf shrub biomass for each species present in each plot by using the point intercept method as described by Wardle et al.[6]. As such, we recorded the total number of times that the vegetation of each species was intercepted by a total of 100 downwardly projected points located throughout the plot. The total number of intercepts for each species was then converted to biomass per unit area through equations previously developed by destructively sampling calibration plots[6]. For bryophytes, we used the approach of Lagerström et al.[7] to determine the biomass of each species, which involved measuring the depth of the live moss layer of each species at each of 15 random points throughout the plot, and converting mean depth to biomass using previously established calibration equations. In the laboratory, total root biomass (shrubs and trees) was estimated in each core used for pyrosequencing by sorting roots out manually; dry weight was then determined by drying at 80°C for 48 h.

Soil C,N,P per area. Gravimetric moisture content of each soil sample was determined after drying (105°C, 48h), and this allowed the calculation of bulk density based on the volume of each soil core. A subsample of soil collected from each plot was then analyzed for total C and N, as well as ^{13}C:^{12}C and ^{15}N:^{14}N ratios on a mass spectrometer (DeltaPlus XP, Thermo Electron, Bremen, Germany) coupled with an elemental analyzer (Flash EA 1112, Thermo Electron). Natural abundance of isotopes is expressed in the δ-notation relative to international standards, Vienna Pee Dee Belemnite for C and atmospheric N_2 for N; δX_{sample} (‰) = 1000 × [(Rsample:Rstandard)-1] where R is the molar ratio of $^{heavy}X$:$^{light}X$ isotope. The standard deviations of isotopic measurements of the working standards used were ± 0.2 ‰ for $\delta^{15}N$ and ± 0.05 ‰ for $\delta^{13}C$. A subsample of soil collected from each plot was analyzed for total C and N using a CHN analyzer (Flash EA 1112,

Thermo Electron, Bremen, Germany). Total P was analyzed by inductively coupled plasma after nitric-perchloric acid digestion (Colorado State University, Boulder, CO, USA). Carbon, N and P were calculated on a per area basis using soil bulk density measurements for each plot.

Mineral nutrients. To assess concentrations of mineral nutrients, another subsample of fresh soil from each plot (5 g dry weight equivalent) was extracted with 50 mL 1 M KCl after shaking for 2 h and frozen (-18°C) and analyzed for NH_4^+, NO_3^-, and PO_4^- by colorimetry on an autoanalyzer III (SEAL Analytical, Kontram OmniProcess AB, Solna, Sweden). In each plot, mixed bed ionic resin capsules (PST1 capsule, Unibest, Bozeman, USA) were buried at 5 cm depth during August 3-18 2014. These were left for one year and harvested over August 3-15 2015 for measurement of NH_4^+, NO_3^-, and PO_4^3-; these measurements were used as an integrated measure of the supply rate of these nutrients from the soil solution[8]. Ionic capsules were extracted using three consecutive rinsings of 10 mL 1 M KCl (30 mL total) and nutrient concentrations were reported on a per capsule basis[9].

Potential microbial activity. Substrate-induced respiration (SIR) was used as an indicator of potential maximum activity of the soil microbial biomass using the method of Anderson and Domsch[10], as modified by Gundale et al.[11]. Each sample (5 g) was placed into a 100-mL glass bottle and adjusted to a water content of 225% (d.w. basis). After water addition, samples were placed in a dark incubator (15°C) overnight to equilibrate. The following day, 2.5 mL of glucose solution (40 g L^{-1}) was pipetted into each bottle, which increased the water content of the soil to ca 250%, and added a quantity of glucose equivalent to 2% soil dry weight. Evolution of CO_2 between 1 and 4 h following glucose addition was then determined by injecting 1 mL subsamples of headspace gas into an infrared gas analyzer.

Decomposition rate. Decomposition rate was assessed by measuring litter mass loss using a standardized substrate (1.5 g d.w.), i.e., *Vaccinium myrtillus* leaf litter (0.96% N, 0.10% P) collected in boreal forest in the Umeå region of Sweden in September 2013. This litter was placed in nylon mesh litter bags (hole size 1.0 × 0.1 mm); two bags were placed in each plot and buried under about 5 cm of humus during August 3-18 2014. Litterbags were left in the plots for one year and harvested in August 2015. At that time, dry weight was determined by drying at 80°C for 48 h and percentage mass loss determined.

Organic matter quality. Organic matter chemistry was quantified by a combination of solid-state cross-polarization magic-angle spinning (CP/MAS) ^{13}C nuclear magnetic resonance (NMR) spectroscopy and mid infra-red (MIR) spectroscopy. First, a calibration set of solid-state ^{13}C NMR spectra were acquired on 60 soil samples selected to provide a strong contrast across the entire dataset (i.e., samples from the control plots with no vegetation removal and the treatment plots with all functional groups removed on all 30 islands) using a Bruker 200 Avance spectrometer (Bruker Corporation, Billerica, MA, USA) equipped with a 4.7 T, 25 wide-bore superconducting magnet operating at a resonance frequency of 50.33 MHz. Operating conditions were identical to those reported in Baldock et al.[12] with the exception that only 5000 scans were obtained for each sample due to the higher C content of the soils in the present study. The proportional allocation of signal intensity to the following seven chemical shift regions (and the C compounds they represent) was determined: 0-45 (Alkyl), 45-60 (N-Alkyl/Methoxyl), 60-95 (O-Alkyl), 95-110 (di-O-Alkyl), 110-145 (Aryl), 145-165 (O-Aryl), 165-190 (Amide/Carboxyl), 190-215 (Ketone)[13]. Diffuse reflectance mid-infrared (MIR) spectra were acquired for all 420 samples using a Thermo Fisher Nicolet 6700 spectrometer (Waltham, MA) equipped with a KBr beam-splitter, a DTGS detector

and an automated diffuse reflectance accessory (Pike Technologies, Madison, WI). For each sample, five replicate subsamples were analyzed by MIR and averaged. Partial least squares regression (PLSR) analyses with full cross validation were used to derive algorithms for predicting the proportional allocation of sample carbon to the various NMR spectral regions using the data acquired for the 60 samples on which NMR analyses were performed[14]. The respective r^2 and RMSEP values derived for each prediction algorithm were: alkyl (r^2 = 0.89 , RMSEP = 1.164), N-alkyl (r^2 = 0.62, RMSEP = 0.264), O-alkyl (r^2 = 0.87, RMSEP = 1.129), di-O-alkyl (r^2 = 0.92, RMSEP = 0.254), aryl (r^2 = 0.71, RMSEP = 0.715), O-aryl (r^2 = 0.71, RMSEP = 0.409), carbonyl (r^2 = 0.38, RMSEP = 0.407) and ketone (r^2 = 0.25, RMSEP = 0.164). The MIR/PLSR prediction algorithms were applied to all 420 samples to provide estimates of the allocation of carbon to each spectral region and thus type of carbon. The alkyl C spectral region is likely dominated by C present in lipids and other aliphatic compounds while the O-alkyl C likely originates from carbohydrates[15]. The alkyl:O-alkyl ratio has been used to provide an index of the extent of decomposition of organic materials, with higher ratios indicating a greater extent of decomposition[16]. The predicted MIR/PLSR proportional allocations of carbon to alkyl and O-alkyl C forms were used to calculate the alkyl:O-alkyl ratio for all 420 samples.

Phospholipid fatty acid. A subsample of soil from each plot was analyzed for its PLFA markers[17] as a measure of microbial biomass of the active microbes[18-20]. After freeze-drying, PLFAs were extracted from each subsample according to the Bligh and Dyer method[21] as modified by White et al.[22]. The abundance of PLFAs was quantified using a Perkin–Elmer Clarus gas chromatograph equipped with a flame ionisation detector (Waltham, MA, USA) and was converted to nmol PLFA per gram of organic matter using conventional nomenclature. We used i14:0, i15:0, a15:0, 15:0, i16:0, 16:1ω9, 16:1ω7c, 16:1ω7t, br17:0, 10me16:0, i17:0, a17:0, 17:1ω8, cy17:0, 17:0, br18:0,

10me17:0, 18:1ω7, 10me18:0, cy19:0 as indicators for bacteria and 18:2ω6 and 18:1ω9 as indicators for fungi[20,23]. The sum of all the PLFA markers was used to represent the active microbial biomass[20].

Nematode density. To assess the effect of biodiversity loss on higher trophic levels of the soil food web, a 100–200 g (wet weight), homogenized, unsieved subsample was used to characterize the nematode density in the soil. This consists of plant- fungal- bacterial- and nematode-feeders and as such provides a measure of the microfaunal consumers supported by the system. Nematodes were extracted by using a sugar flotation method (modified from Jenkins 1964). Nematodes were heat-killed and fixed using 35% formaldehyde diluted to 4%. Subsequently, for each soil sample, nematode density was calculated per unit soil weight.

Supplementary Table 1 | Variability in soil and vegetation parameters (mean ± SE, *n* = 10) across the island size classes[7,24-28].

Ecosystem properties	Island size		
	Large	Medium	Small
Size (min – max) (ha)	1.1 – 15.0	0.13 – 0.90	0.02 – 0.10
Time since last fire (years)	585 ± 233	2180 ± 385	3250 ± 439
Standing plant biomass (g m^{-2})	9349 ± 485	8340 ± 877	3470 ± 470
Dominant tree species	*Pinus sylvestris*	*Betula pubescens*	*Picea abies*
Dominant shrub species	*Vaccinium myrtillus*	*Vaccinium vitis-idaea*	*Empetrum hermaphroditum*
Net primary productivity (g m^{-2} yr^{-1})	256 ± 14	247 ± 12	159 ± 18
Carbon stock (kg m^2)	6.22 ± 2.16	13.17 ± 6.16	22.43± 6.74
Mineral N (µg N g^{-1})	38.2 ± 14.4	58.1 ± 9.2	25.3 ± 8.0
Dissolved organic N (µg N g)	39.1 ± 7.2	50.7 ± 5.5	40.3 ± 4.6
Mineral P (µg P g^{-1})	43.6 ± 4.9	37.7 ± 4.3	24.4 ± 2.3
Membrane-extractable P (mmol/kg)	5.9 ± 0.7	6.5 ± 0.4	4.9 ± 0.3
Humus C to N ratio	40.4 ± 1.18	36.0 ± 1.17	32.9 ± 0.79
Humus C to P ratio	623 ± 20	687 ± 36	759 ± 30
Humus N to P ratio	15.4 ± 0.5	19.1 ± 0.9	23.3 ± 1.1
pH	3.51 ± 0.029	3.42 ± 0.027	3.38 ± 0.039

Supplementary Table 2 | The 15 individual ecosystem functions and properties used for calculating ecosystem multifunctionality. Categories, methods, units and a brief description are given for each ecosystem function. C = carbon, N = nitrogen, P = phosphorus, KCl = potassium chloride, NMR = nuclear magnetic resonance, PLFA = phospholipid fatty acid.

Ecosystem functions and properties	Categories	Methods	Units	Description
Soil N per area	N cycling	CHN analyzer	g N m^{-2}	The total amount of N in the soil on an areal basis, which interacts with many biotic and abiotic components of the ecosystem[29,30]
Soil mineral N	N cycling	KCl extraction	mg N m^{-2}	The fraction of the soil N pool that is most readily available for plant and microbial uptake[31,32]
Soil exchangeable N	N cycling	Ionic resin capsules	µg N per capsule $year^{-1}$	An integrative measurement of the supply rate of mineral N from the soil and an indicator of less conservative N cycling[8,11]
Soil P per area	P cycling	Acid digestion	g P m^{-2}	The total amount of P in the soil on an areal basis, which interacts with many biotic and abiotic components of the ecosystem[33-35]
Soil mineral P	P cycling	KCl extraction	mg P m^{-2}	The fraction of the soil P pool that is most readily available for plant and microbial uptake[36-38]
Soil exchangeable P	P cycling	Ionic resin capsules	µg P per capsule $year^{-1}$	An integrative measurement of the supply rate of mineral P from the soil and an indicator of less conservative P cycling [39]
Soil C per area	C cycling	CHN analyzer	g C m^{-2}	The total amount of C in the soil on an areal basis, which interacts with many biotic and abiotic components of the ecosystem[28,40,41]
Decomposition rate	C cycling	Litter mass loss	%mass loss $year^{-1}$	The fraction of fresh organic matter that is decomposed by soil communities; indicative of the activity of the microbial community and its capacity to drive C turnover in terrestrial ecosystem[42,43]
Soil alkyl:O-alkyl ratio	C cycling	NMR spectra	unitless	Indicator of OM quality and microbial processing, with higher ratios indicating losses of more labile C relative to more stable C compounds[13,15]
Shrub biomass	Plant functioning	Point intercept and allometric equations	g m^{-2}	Aboveground biomass of ericaceous shrub species, indicative of productivity of the understorey vegetation in this study system[6,27]
Root biomass	Plant functioning	Direct estimation	mg kg^{-1}	The belowground biomass of vascular plants, indicative of plant belowground resource inputs in this study system[27,28]
Moss biomass	Plant functioning	Depth measurement and allometric equations	g m^{-2}	Biomass of all bryophytes, indicative of moss productivity and associative N_2 fixation in this study system[7,27,44]
Potential microbial activity	Soil functioning	Substrate induced respiration	µg CO_2 g^{-1} soil h^{-1}	A measure of the maximum potential activity of the component of the microbial community that is responsible for driving decomposition and related processes[10,45]
Active microbial biomass	Soil functioning	Microbial PLFA	nmol PLFA g^{-1} soil	An indicator of the active microbial biomass, i.e., the component of the microbial community that is active in driving biogeochemical cycling[18-20]
Nematode density	Soil functioning	Extraction and counting	number g^{-1} soil	Total density of a major group of consumer organisms that collectively graze on fungi, bacteria and roots, thereby accelerating turnover, nutrient mineralization and soil functioning[46-48]

Supplementary Table 3 | Results from full factorial mixed linear models to test for the effects of species removals (**a**) and functional group removals (**b**) classified in 3 categories: 'Main effects', 'Interactions' (i.e., interactive effects among removal treatments) and 'Context-dependency' (i.e., interactive effects between removal treatments and island size class) on 15 ecosystem functions and properties. Dark-blue boxes and light-blue indicate significant ($P < 0.05$) and marginally significant effects ($0.05 < P < 0.10$).

a - Species Removals	Main effects				Interactions				Context-dependency						
	Island size (IS)	*Vaccinium myrtillus removal* (-Vm)	*Vaccinium vitis-idaea removal* (-Vv)	*Empetrum hermaphroditum* removal (-Eh)	-Vm × -Vv	-Vm × -Eh	-Vv × -Eh	-Vm × -Vv × -Eh	IS × -Vm	IS × -Vv	IS × -Eh	IS × -Vm × -Vv	IS × -Vm × -Eh	IS × -Vv × -Eh	IS × -Vm × -Vv × -Eh
Soil N per area															
Soil mineral N															
Soil exchangeable N															
Soil P per area															
Soil mineral P															
Soil exchangeable P															
Soil C per area															
Decomposition rate															
Soil alkyl:O-alkyl ratio															
Shrub biomass															
Root biomass															
Moss biomass															
Potential microbial activity															
Active microbial biomass															
Nematode density															

b - Functional Group Removals	Main effects				Interactions				Context-dependency						
	Island size (IS)	Tree roots removal (-T)	Mosses removal (-M)	Shrubs removal (-S)	-T × -M	-T × -S	-M × -S	-T × -M × -S	IS × -T	IS × -M	IS × -S	IS × -T × -M	IS × -T × -S	IS × -M × -S	IS × -T × -M × -S
Soil N per area															
Soil mineral N															
Soil exchangeable N															
Soil P per area															
Soil mineral P															
Soil exchangeable P															
Soil C per area															
Decomposition rate															
Soil alkyl:O-alkyl ratio															
Shrub biomass															
Root biomass															
Moss biomass															
Potential microbial activity															
Active microbial biomass															
Nematode density															

Supplementary Table 4 | Heat map of the relative effects of species removals (**a**) and functional group removals (**b**) across island size classes (large, medium and small) on each of the 15 individual functions. Removal treatments involve removals of *Vaccinium myrtillus* (-Vm) *Vaccinium vitis-idaea* (-Vv), *Empetrum hermaphroditum* (-Eh), trees (-T), shrubs (-S), and mosses (-M). The effects of plant removals varied from negative (shades of red) to positive (shades of blue), and these effects sometimes interacted with ecosystem type (see Supplementary Table 3 for model results). Overall, -Vm and -M had larger impacts on large islands, -Vv and -T had larger impacts on medium islands, -Eh and -S had larger impacts on small islands.

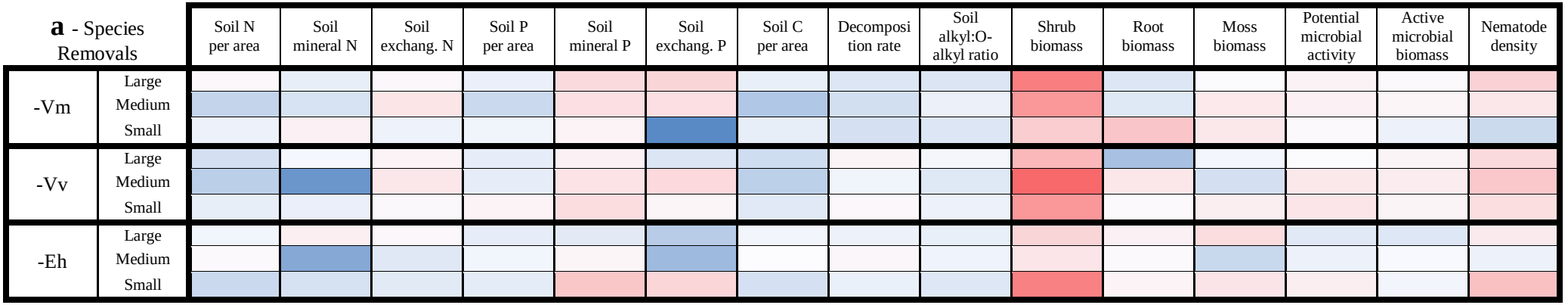

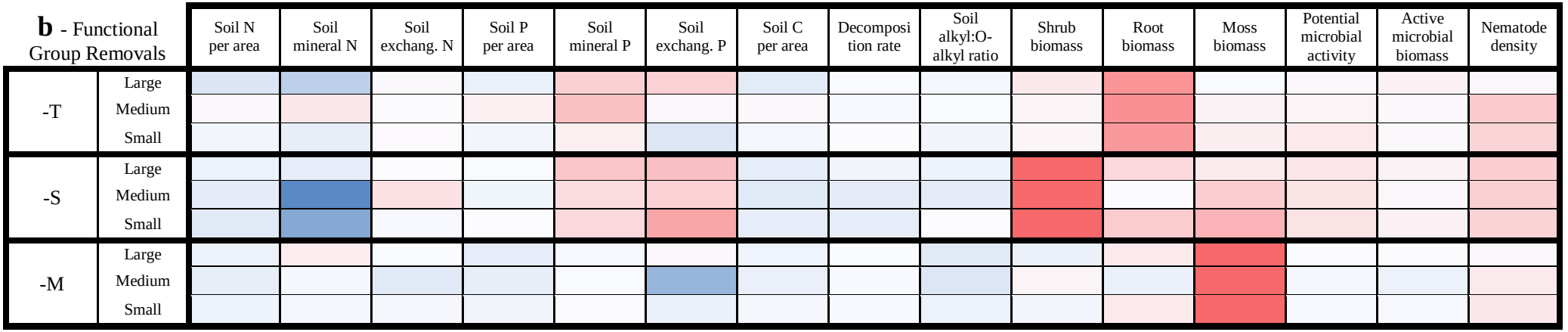

Supplementary Table 5 | Results from full factorial mixed linear models to test for the effects of species removals (**a**), and functional group removals (**b**) on ecosystem multifunctionality. Values in bold indicate significant differences at $P < 0.05$. Multifunctionality was calculated as the mean of all 15 individual functions and properties standardized to a common scale (see M&M).

a - Species removals	numDF	denDF	F value	*P-value*
Island size class (IS)	2	27	3.81	**0.035**
Vaccinium myrtillus removal (-Vm)	1	189	19.97	**<.0001**
Vaccinium vitis-idaea removal (-Vv)	1	189	34.30	**<.0001**
Empetrum hermaphroditum removal (-Eh)	1	189	11.24	**0.001**
IS × -Vm	2	189	1.56	0.21
IS × -Vv	2	189	1.30	0.28
-Vm × -Vv	1	189	0.98	0.32
IS × -Eh	2	189	2.61	0.077
-Vm × -Eh	1	189	5.52	**0.020**
-Vv × -Eh	1	189	3.16	0.077
IS × -Vm × -Vv	2	189	0.36	0.70
IS × -Vm × -Eh	2	189	0.00	1.00
IS × -Vv × -Eh	2	189	0.71	0.50
-Vm × -Vv × -Eh	1	189	0.88	0.35
IS × -Vm × -Vv × -Eh	2	189	0.88	0.42

b - Functional group removals	numDF	denDF	F value	*P-value*
Island size class (IS)	2	27	2.67	0.088
Tree root removal (-T)	1	189	43.86	**<.0001**
Moss removal (-M)	1	189	10.18	**0.002**
Shrub removal (-S)	1	189	149.06	**<.0001**
IS × -T	2	189	2.95	0.055
IS × -M	2	189	0.86	0.43
-T × -M	1	189	1.49	0.22
ISC × -S	2	189	1.72	0.18
-T × -S	1	189	1.49	0.22
-M × -S	1	189	1.40	0.24
IS × -T × -M	2	189	0.16	0.85
IS × -T × -S	2	189	2.73	0.068
IS × -M × -S	2	189	0.58	0.56
-T × -M × -S	1	189	0.32	0.57
IS × -T × -M × -S	2	189	1.33	0.27

Supplementary Table 6 | PERMANOVA results (n = 9999) evaluating the effects of species removals (**a**) and functional group removals (**b**) on fungal community structure based on Bray-Curtis distances of fungal OTUs. Values in bold indicate significant differences at $P < 0.05$. Island identity was included in the model to account for the natural variation among ecosystems and permutations were constrained within each island. OTUs that do not reach 0.01% as their maximum relative abundance were removed prior to the analysis.

a - Species removals	DF	Sum Squares	Mean Squares	F value	*P-value*
Island size class (IS)	2	2.82	1.41	8.43	**<0.001**
Vaccinium myrtillus removal (-Vm)	1	0.29	0.29	1.71	**0.012**
Vaccinium vitis-idaea removal (-Vv)	1	0.48	0.48	2.87	**<0.001**
Empetrum hermaphroditum removal (-Eh)	1	0.28	0.28	1.65	**0.019**
IS × -Vm	2	0.34	0.17	1.03	0.40
IS × -Vv	2	0.33	0.16	0.98	0.49
-Vm × -Vv	1	0.13	0.13	0.78	0.82
IS × -Eh	2	0.33	0.16	0.97	0.52
-Vm × -Eh	1	0.21	0.21	1.25	0.15
-Vv × -Eh	1	0.16	0.16	0.98	0.49
IS × -Vm × -Vv	2	0.45	0.22	1.34	**0.043**
IS × -Vm × -Eh	2	0.38	0.19	1.12	0.24
IS × -Vv × -Eh	2	0.42	0.21	1.26	0.087
-Vm × -Vv × -Eh	1	0.28	0.28	1.67	**0.014**
IS × -Vm × -Vv × -Eh	2	0.34	0.17	1.02	0.43

b - Functional group removals	DF	Sum Squares	Mean Squares	F value	*P-value*
Island size class (IS)	2	3.04	1.52	9.31	**<0.001**
Tree root removal (-T)	1	0.32	0.32	1.95	**0.009**
Moss removal (-M)	1	0.61	0.61	3.73	**<0.001**
Shrub removal (-S)	1	2.81	2.81	17.19	**<0.001**
IS × -T	2	0.51	0.26	1.57	**0.012**
IS × -M	2	0.33	0.17	1.01	0.41
-T × -M	1	0.16	0.16	0.97	0.48
IS × -S	2	0.44	0.22	1.33	0.073
-T × -S	1	0.21	0.21	1.27	0.15
-M × -S	1	0.42	0.42	2.56	**<0.001**
IS × -T × -M	2	0.28	0.14	0.85	0.76
IS × -T × -S	2	0.26	0.13	0.79	0.86
IS × -M × -S	2	0.32	0.16	0.98	0.50
-T × -M × -S	1	0.16	0.16	0.99	0.45
IS × -T × -M × -S	2	0.24	0.12	0.73	0.93

Supplementary Table 7 | List of OTUs depleted as a consequence of the removal of all shrubs in the functional group removal experiment. A complete description (Phylum, Subphylum, Class, Order, Family, Genus, Species) and the associated putative functional group are given for each cluster when available.

Name	Phylum	Subphylum	Class	Order	Family	Genus	Species	Known	Putative
FUNGI3	Ascomycota	Pezizomycotina	Leotiomycetes	Helotiales	Helotiaceae	Rhizoscyphus	Rhizoscyphus.eric	ERI	ERI
FUNGI114	Ascomycota	Pezizomycotina	Leotiomycetes	Helotiales	Helotiaceae	Rhizoscyphus	UNK	UNK	ERI
FUNGI0	Ascomycota	Pezizomycotina	Eurotiomycetes	Chaetothyriales	UNK	UNK	UNK	UNK	ERI
FUNGI304	Ascomycota	Pezizomycotina	Leotiomycetes	Helotiales	Hyaloscyphaceae	UNK	UNK	UNK	ERI
FUNGI75	Ascomycota	Pezizomycotina	Leotiomycetes	UNK	Myxotrichaceae	Oidiodendron	Oidiodendron.mai	ERI	ERI
FUNGI169	Ascomycota	Pezizomycotina	Leotiomycetes	Helotiales	UNK	UNK	UNK	UNK	ERI
FUNGI234	Ascomycota	Pezizomycotina	Leotiomycetes	Helotiales	Vibrisseaceae	Acephala	UNK	UNK	ERI
FUNGI186	Basidiomycota	Agaricomycotina	Agaricomycetes	Sebacinales	Sebacinaceae	Sebacina	UNK	UNK	ERI
FUNGI316	Ascomycota	Pezizomycotina	Leotiomycetes	Helotiales	Dermateaceae	Cryptosporiopsis	UNK	ERI	ERI
FUNGI295	Ascomycota	Pezizomycotina	Leotiomycetes	Helotiales	UNK	UNK	UNK	UNK	ERI
FUNGI115	Ascomycota	Pezizomycotina	Leotiomycetes	Helotiales	Helotiaceae	Rhizoscyphus	UNK	UNK	ERI
FUNGI158	Ascomycota	Pezizomycotina	Leotiomycetes	Helotiales	Dermateaceae	Cryptosporiopsis	UNK	UNK	ERI
FUNGI58	Ascomycota	Pezizomycotina	Leotiomycetes	Helotiales	UNK	UNK	UNK	UNK	ROOT
FUNGI60	Ascomycota	Pezizomycotina	Leotiomycetes	Helotiales	Dermateaceae	Mollisia	Mollisia.minutella	ROOT	ROOT
FUNGI5	Ascomycota	Taphrinomycotina	Archaeorhizomyce	UNK	UNK	UNK	UNK	UNK	ROOT
FUNGI257	Ascomycota	Pezizomycotina	Leotiomycetes	Helotiales	UNK	UNK	UNK	UNK	ROOT
FUNGI48	Ascomycota	Taphrinomycotina	Archaeorhizomyce	UNK	UNK	UNK	UNK	UNK	ROOT
FUNGI225	Ascomycota	Pezizomycotina	Leotiomycetes	Helotiales	UNK	UNK	UNK	UNK	ROOT
FUNGI40	Ascomycota	Taphrinomycotina	Archaeorhizomyce	UNK	UNK	UNK	UNK	UNK	ROOT
FUNGI416	Ascomycota	Pezizomycotina	Leotiomycetes	Helotiales	UNK	UNK	UNK	UNK	ROOT
FUNGI313	Ascomycota	Pezizomycotina	Leotiomycetes	Helotiales	UNK	Meliniomyces	UNK	UNK	ROOT
FUNGI71	Ascomycota	Pezizomycotina	Leotiomycetes	Helotiales	Hyaloscyphaceae	Cistella	UNK	UNK	ROOT
FUNGI236	Basidiomycota	Agaricomycotina	Agaricomycetes	Sebacinales	Sebacinaceae	Sebacina	UNK	UNK	ROOT
FUNGI227	Basidiomycota	Agaricomycotina	Agaricomycetes	Cantharellales	Ceratobasidiaceae	Ceratobasidium	UNK	UNK	ROOT
FUNGI21	Basidiomycota	Agaricomycotina	Agaricomycetes	Trechisporales	Hydnodontaceae	Trechispora	UNK	SAP	SAP
FUNGI52	Ascomycota	Pezizomycotina	Leotiomycetes	Helotiales	Hyaloscyphaceae	Mollisina	UNK	SAP	SAP
FUNGI80	Ascomycota	Pezizomycotina	Leotiomycetes	Helotiales	Hyaloscyphaceae	Lachnum	UNK	SAP	SAP
FUNGI28	Basidiomycota	Agaricomycotina	Agaricomycetes	Agaricales	Mycenaceae	Mycena	Mycena.claviculari	SAP	SAP
FUNGI661	Ascomycota	Pezizomycotina	Leotiomycetes	Helotiales	Hyaloscyphaceae	UNK	UNK	UNK	SAP
FUNGI224	Ascomycota	Pezizomycotina	Eurotiomycetes	Chaetothyriales	Herpotrichiellacea	Cladophialophora	UNK	SAP	SAP
FUNGI178	Basidiomycota	Agaricomycotina	Agaricomycetes	Agaricales	Clavariaceae	UNK	UNK	UNK	SAP
FUNGI431	Ascomycota	Pezizomycotina	Leotiomycetes	Helotiales	Hyaloscyphaceae	Cistella	UNK	UNK	SAP
FUNGI64	Basidiomycota	Agaricomycotina	Agaricomycetes	Agaricales	Mycenaceae	Mycena	Mycena.monticola	SAP	SAP
FUNGI275	Ascomycota	Pezizomycotina	Sordariomycetes	Chaetosphaeriales	Chaetosphaeriacea	Chaetosphaeria	UNK	SAP	SAP
FUNGI50	Ascomycota	Pezizomycotina	Pezizomycetes	Pezizales	Sarcosomataceae	Pseudoplectania	UNK	SAP	SAP
FUNGI489	Ascomycota	Pezizomycotina	Dothideomycetes	Venturiales	Sympoventuriacea	Scolecobasidium	UNK	SAP	SAP
FUNGI563	Ascomycota	Pezizomycotina	Eurotiomycetes	Chaetothyriales	Herpotrichiellacea	Cladophialophora	UNK	SAP	SAP
FUNGI205	Ascomycota	Pezizomycotina	Leotiomycetes	Helotiales	Hyaloscyphaceae	Lachnum	UNK	SAP	SAP
FUNGI23	Ascomycota	Pezizomycotina	Leotiomycetes	Helotiales	UNK	Chalara	Chalara.holubovae	SAP	SAP
FUNGI147	Ascomycota	Pezizomycotina	Sordariomycetes	Sordariales	Cephalothecaceae	Phialemonium	UNK	SAP	SAP
FUNGI66	Ascomycota	Pezizomycotina	Leotiomycetes	Helotiales	UNK	Coleophoma	Coleophoma.eucal	SAP	SAP
FUNGI200	Ascomycota	Pezizomycotina	Leotiomycetes	Helotiales	Helotiaceae	Hymenoscyphus	UNK	SAP	SAP
FUNGI396	Ascomycota	Pezizomycotina	Eurotiomycetes	Chaetothyriales	Herpotrichiellacea	Exophiala	UNK	SAP	SAP
FUNGI72	Ascomycota	Pezizomycotina	Leotiomycetes	Helotiales	Hyaloscyphaceae	Calycina	UNK	SAP	SAP
FUNGI101	Basidiomycota	Agaricomycotina	Agaricomycetes	Agaricales	Mycenaceae	Mycena	Mycena.thymicola	SAP	SAP
FUNGI454	Ascomycota	Pezizomycotina	Leotiomycetes	Helotiales	Helotiaceae	Hevderia	UNK	SAP	SAP
FUNGI385	Ascomycota	Pezizomycotina	Dothideomycetes	Venturiales	Sympoventuriacea	(Sympoventuria)	UNK	UNK	SAP
FUNGI96	Ascomycota	Pezizomycotina	Dothideomycetes	Venturiales	Sympoventuriacea	Scolecobasidium	UNK	SAP	SAP
FUNGI318	Basidiomycota	Agaricomycotina	Agaricomycetes	Cantharellales	Ceratobasidiaceae	Ceratobasidium	UNK	UNK	SAP
FUNGI282	Basidiomycota	Agaricomycotina	Agaricomycetes	Agaricales	Clavariaceae	UNK	UNK	UNK	SAP
FUNGI79	Ascomycota	Pezizomycotina	Leotiomycetes	Helotiales	Hyaloscyphaceae	Mycoarthris	UNK	SAP	SAP
FUNGI354	Ascomycota	Pezizomycotina	Leotiomycetes	Helotiales	Helotiaceae	UNK	UNK	UNK	SAP
FUNGI223	Ascomycota	Pezizomycotina	Leotiomycetes	Helotiales	Hyaloscyphaceae	Arachnopeziza	UNK	SAP	SAP
FUNGI239	Ascomycota	Pezizomycotina	Leotiomycetes	Helotiales	Helotiaceae	Hymenoscyphus	UNK	SAP	SAP
FUNGI184	Ascomycota	Pezizomycotina	Leotiomycetes	Helotiales	Hyaloscyphaceae	Lachnellula	UNK	SAP	SAP
FUNGI191	Ascomycota	Pezizomycotina	Dothideomycetes	Pleosporales	Lophiostomataceae	Lophiostoma	UNK	SAP	SAP
FUNGI254	Ascomycota	Pezizomycotina	Leotiomycetes	Helotiales	UNK	Chalara	Chalara.holubovae	SAP	SAP
FUNGI126	Ascomycota	Pezizomycotina	Leotiomycetes	Helotiales	UNK	UNK	UNK	UNK	ECMcon
FUNGI245	Ascomycota	Pezizomycotina	Leotiomycetes	Helotiales	Dermateaceae	UNK	UNK	UNK	ECMcon
FUNGI142	Basidiomycota	Agaricomycotina	Agaricomycetes	Thelephorales	Thelephoraceae	Tomentella	Tomentella.sublila	ECMsmo	ECMsmo
FUNGI297	Ascomycota	Pezizomycotina	Lecanoromycetes	Pertusariales	Ochrolechiaceae	Ochrolechia	UNK	LICHEN	LICHEN
FUNGI195	Ascomycota	Pezizomycotina	Lecanoromycetes	Lecanorales	Cladoniaceae	Cladonia	UNK	LICHEN	LICHEN
FUNGI98	Ascomycota	Pezizomycotina	Lecanoromycetes	Ostropales	UNK	UNK	UNK	LICHEN	LICHEN
FUNGI13	Ascomycota	Pezizomycotina	Eurotiomycetes	Eurotiales	Trichocomaceae	Penicillium	Penicillium.spinul	MOULD	MOULD
FUNGI220	Basal lineages	Mucoromycotina	Mucoromycetes	Mortierellales	Mortierellaceae	Mortierella	Mortierella.minutis	MOULD	MOULD
FUNGI467	Ascomycota	Pezizomycotina	Sordariomycetes	Hypocreales	Niessliaceae	Eucasphaeria	UNK	MOULD	MOULD
FUNGI456	Ascomycota	Pezizomycotina	Sordariomycetes	Hypocreales	Niessliaceae	Eucasphaeria	UNK	MOULD	MOULD
FUNGI36	Ascomycota	Pezizomycotina	Dothideomycetes	Venturiales	Venturiaceae	Venturia	Venturia.inequalis	PATHO	PATHO
FUNGI20	Ascomycota	Pezizomycotina	Leotiomycetes	Helotiales	Phacidiaceae	Ceuthospora	Ceuthospora.pinast	PATHO	PATHO
FUNGI180	Ascomycota	Pezizomycotina	Leotiomycetes	Helotiales	Dermateaceae	Neofabraea	UNK	PATHO	PATHO
FUNGI352	Basidiomycota	Ustilaginomycotin	Exobasidiomycete	Exobasidiales	Exobasidiaceae	Exobasidium	Exobasidium.aresc	PATHO	PATHO
FUNGI141	Ascomycota	Pezizomycotina	Dothideomycetes	Dothideales	Dothideaceae	Endoconidioma	Endoconidioma.po	UNK	PATHO
FUNGI527	Ascomycota	Pezizomycotina	Dothideomycetes	Venturiales	Venturiaceae	Cylindrosympodiu	UNK	PATHO	PATHO
FUNGI208	Ascomycota	Pezizomycotina	Dothideomycetes	Capnodiales	Teratosphaeriaceae	Hortaea	UNK	PATHO	PATHO
FUNGI132	Ascomycota	Pezizomycotina	Sordariomycetes	Xylariales	Amphisphaeriacea	Seiridium	UNK	PATHO	PATHO
FUNGI148	Ascomycota	Pezizomycotina	Sordariomycetes	Diaportales	Gnomoniaceae	Gnomonia	UNK	PATHO	PATHO
FUNGI545	Ascomycota	Pezizomycotina	Dothideomycetes	Capnodiales	Teratosphaeriaceae	Devriesia	UNK	UNK	PATHO
FUNGI375	Ascomycota	Pezizomycotina	Dothideomycetes	Venturiales	Venturiaceae	Cylindrosympodiu	UNK	PATHO	PATHO
FUNGI81	Ascomycota	Pezizomycotina	Sordariomycetes	Xylariales	Amphisphaeriacea	Polyscytalum	UNK	PATHO	PATHO
FUNGI249	Ascomycota	Pezizomycotina	Dothideomycetes	Botryosphaeriales	UNK	UNK	UNK	UNK	PATHO
FUNGI68	Basidiomycota	Agaricomycotina	Tremellomycetes	Cystofilobasidiales		Syzygospora	Syzygospora.effib	YEAST	YEAST
FUNGI157	Basidiomycota	Pucciniomycotina	Microbotryomycet	UNK	UNK	UNK	UNK	YEAST	YEAST
FUNGI100	Basidiomycota	Agaricomycotina	Tremellomycetes	Cystofilobasidiales	UNK	UNK	Cystofilobasidiales	YEAST	YEAST
FUNGI108	Basidiomycota	Agaricomycotina	Tremellomycetes	Tremellales	Trichosporonaceae	Trichosporon	Trichosporon.poro	YEAST	YEAST
FUNGI487	Ascomycota	Pezizomycotina	Dothideomycetes	UNK	UNK	(Cladoriella)	UNK	UNK	UNK
FUNGI51	Ascomycota	Pezizomycotina	Leotiomycetes	UNK	UNK	Gorgomyces	UNK	UNK	UNK
FUNGI324	Ascomycota	Pezizomycotina	Leotiomycetes	Helotiales	UNK	UNK	UNK	UNK	UNK
FUNGI448	Fungi	UNK	UNK	UNK	UNK	UNK	UNK	UNK	UNK
FUNGI310	Ascomycota	Pezizomycotina	Dothideomycetes	UNK	UNK	UNK	UNK	UNK	UNK
FUNGI468	Ascomycota	Pezizomycotina	Leotiomycetes	Helotiales	Dermateaceae	UNK	UNK	UNK	UNK
FUNGI31	Ascomycota	Pezizomycotina	Leotiomycetes	Helotiales	Dermateaceae	UNK	UNK	UNK	UNK
FUNGI481	Ascomycota	Pezizomycotina	Leotiomycetes	Helotiales	UNK	UNK	UNK	UNK	UNK
FUNGI493	non ident	non ident	non ident	non ident	non ident	non ident	non ident	non ident	non ident
FUNGI596	non ident	non ident	non ident	non ident	non ident	non ident	non ident	non ident	non ident
FUNGI656	non ident	non ident	non ident	non ident	non ident	non ident	non ident	non ident	non ident
FUNGI698	non ident	non ident	non ident	non ident	non ident	non ident	non ident	non ident	non ident
FUNGI748	non ident	non ident	non ident	non ident	non ident	non ident	non ident	non ident	non ident

Supplementary Table 8 | Results from full factorial mixed linear models to test for the effects of plant functional group removals, island size class and their interactions on estimated fungal species richness (α-diversity) (**a**), total fungal relative biomass (**b**) and the fungal to bacterial ratio (**c**). Values in bold indicate significant differences at $P < 0.05$.

a - Estimated species richness	numDF	denDF	F value	*P-value*
Island size class (IS)	2	27	3.35	0.05
Tree root removal (-T)	1	187	0.00	0.96
Moss removal (-M)	1	187	0.03	0.86
Shrub removal (-S)	1	187	20.42	**<.0001**
IS × -T	2	187	0.16	0.86
IS × -M	2	187	1.39	0.25
-T × -M	1	187	0.37	0.54
IS × -S	2	187	1.77	0.17
-T × -S	1	187	0.08	0.78
-M × -S	1	187	0.00	1.00
IS × -T × -M	2	187	0.56	0.57
IS × -T × -S	2	187	0.75	0.48
IS × -M × -S	2	187	0.15	0.86
-T × -M × -S	1	187	0.32	0.57
IS × -T × -M × -S	2	187	0.19	0.83

b - Total fungal relative biomass	numDF	denDF	F value	*P-value*
Island size class (IS)	2	27	1.73	0.20
Tree root removal (-T)	1	186	33.74	**<.0001**
Moss removal (-M)	1	186	0.78	0.38
Shrub removal (-S)	1	186	95.31	**<.0001**
IS × -T	2	186	0.55	0.58
IS × -M	2	186	0.39	0.68
-T × -M	1	186	1.39	0.24
IS × -S	2	186	0.10	0.91
-T × -S	1	186	0.03	0.87
-M × -S	1	186	0.41	0.52
IS × -T × -M	2	186	0.19	0.83
IS × -T × -S	2	186	0.00	1.00
IS × -M × -S	2	186	0.82	0.44
-T × -M × -S	1	186	1.29	0.26
IS × -T × -M × -S	2	186	1.38	0.26

c - Fungal to bacterial ratio	numDF	denDF	F value	*P-value*
Island size class (IS)	2	27	2.00	0.16
Tree root removal (-T)	1	186	18.22	**<.0001**
Moss removal (-M)	1	186	2.84	0.09
Shrub removal (-S)	1	186	94.75	**<.0001**
IS × -T	2	186	0.29	0.75
IS × -M	2	186	0.05	0.95
-T × -M	1	186	0.00	0.99
IS × -S	2	186	0.53	0.59
-T × -S	1	186	1.00	0.32
-M × -S	1	186	0.04	0.84
IS × -T × -M	2	186	0.12	0.89
IS × -T × -S	2	186	1.66	0.19
IS × -M × -S	2	186	0.46	0.64
-T × -M × -S	1	186	0.01	0.93
IS × -T × -M × -S	2	186	1.17	0.31

Supplementary Table 9 | Results of the linear mixed effects models to test for the effects of plant diversity, fungal diversity and environmental parameters on ecosystem multifunctionality for the species removal experiment (**a**), and the functional group removal experiment (**b**). Additional explanatory variables were added as co-variables to the most parsimonious model to assess whether diversity effects were still present when potentially co-varying variables were accounted for. Explanatory variables were all centered and standardized prior to the analysis. The notation (1|variable) corresponds to the random intercept of the selected parameter (see Mori et al.[49]). Values in bold indicate significant differences at $P < 0.05$. AIC: Akaike's Information Criterion. *Data from Wardle et al.[6].

a - Species removal experiment	AIC	Plant diversity (*P-value*)	Fungal diversity (*P-value*)
Model selected			
Multifunctionality ~ Plant diversity + Fungal diversity + (1|Island identity)	-724.50	**<0.001**	**0.034**
Parameter added to the best model selected			
+ (1|Vm-removal) + (1|Vv-removal) + (1|Eh-removal)	-718.59	**<0.001**	**0.031**
+ (1|Island size)	-723.96	**<0.001**	**0.035**
+ C14-age for time since last fire*	-725.85	**<0.001**	**0.023**
+ Soil water content	-707.81	**<0.001**	0.062
+ Soil ^{15}N	-726.77	**<0.001**	**0.035**
+ Soil ^{13}C	-730.09	**<0.001**	**0.029**
+ Soil C:N ratio	-724.90	**<0.001**	**0.046**
b - Functional group removal experiment	AIC	Plant diversity (*P-value*)	Fungal diversity (*P-value*)
Model selected			
Multifunctionality ~ Plant diversity + Fungal diversity + (1|Island identity)	-733.43	**<0.001**	**<0.001**
Parameter added to the best model selected			
+ (1|Tree-removal) + (1|Moss-removal) + (1|Shrub-removal)	-743.40	**0.005**	**0.003**
+ (1|Island size)	-731.51	**<0.001**	**<0.001**
+ C14-age for time since last fire*	-737.07	**<0.001**	**<0.001**
+ Soil water content	-734.48	**<0.001**	**<0.001**
+ Soil ^{15}N	-736.84	**<0.001**	**<0.001**
+ Soil ^{13}C	-736.25	**<0.001**	**0.001**
+ Soil C:N ratio	-731.48	**<0.001**	**<0.001**

Supplementary Table 10 | Results of the linear mixed effects models to test for the effects of plant diversity, fungal diversity and environmental parameters on ecosystem multifunctionality for the species removal experiment (**a**), and the functional group removal experiment (**b**). In this analysis, ecosystem multifunctionality is based on the mixed effects fit across different functions. Additional explanatory variables were added as co-variables to the most parsimonious model to assess whether diversity effects were still present when potentially co-varying variables were accounted for. Explanatory variables were all centered and standardized prior to the analysis. The notation (1|variable) corresponds to the random intercept of the selected parameter (see Mori et al.[49]). Equivalent results were obtained from the analyses excluding the random intercept of (1|Function). Values in bold indicate significant differences at $P < 0.05$. AIC: Akaike's Information Criterion. *Data from Wardle et al.[6].

a - Species removal experiment	AIC	Plant diversity (*P-value*)	Fungal diversity (*P-value*)
Model selected			
Multifunctionality			
~ Plant diversity + Fungal diversity + (1|Island identity) + (1|Function)	-2336.2	**<0.001**	**0.031**
Parameter added to the best model selected			
+ (1|Vm-removal) + (1|Vv-removal) + (1|Eh-removal)	-2330.9	**<0.001**	**0.027**
+ (1|Island size)	-2337.1	**<0.001**	**0.031**
+ C14-age for time since last fire*	-2337.9	**<0.001**	**0.020**
+ Soil water content	-2342.0	**<0.001**	0.062
+ Soil ^{15}N	-2337.6	**<0.001**	**0.032**
+ Soil ^{13}C	-2343.0	**<0.001**	**0.025**
+ Soil C:N ratio	-2336.6	**<0.001**	**0.041**
b - Functional group removal experiment	AIC	Plant diversity (*P-value*)	Fungal diversity (*P-value*)
Model selected			
Multifunctionality			
~ Plant diversity + Fungal diversity + (1|Island identity) + (1|Function)	-2350.1	**<0.001**	**<0.001**
Parameter added to the best model selected			
+ (1|Tree-removal) + (1|Moss-removal) + (1|Shrub-removal)	-2363.8	**0.013**	**0.004**
+ (1|Island size)	-2348.8	**<0.001**	**<0.001**
+ C14-age for time since last fire*	-2354.6	**<0.001**	**<0.001**
+ Soil water content	-2351.4	**<0.001**	**<0.001**
+ Soil ^{15}N	-2353.1	**<0.001**	**<0.001**
+ Soil ^{13}C	-2353.9	**<0.001**	**0.001**
+ Soil C:N ratio	-2348.2	**<0.001**	**<0.001**

Supplementary Fig. 1 | Photos depicting the study system: (**a**) Overview of the study system in Lake Hornavan, (**b**) Example of removal plot after 19 years of shrub removals (left) versus the control (right), (**c**) Mycorrhizal network (white) developing in the humus layer. Photos representing the different island size classes along the islands chronosequence: (**d**) large island, (**e**) medium island, and (**f**) small island. Photos representing the typical vegetation on these different island size classes: (**g**) *Pinus sylvestris* and *Vaccinium myrtillus*, characteristic of large islands, (**h**) *Betula pubescens* and *Vaccinium vitis-idaea*, characteristic of medium islands, (**i**) *Picea abies* and *Empetrum hermaphroditum*, characteristic of small islands (Photo credits: N. Fanin).

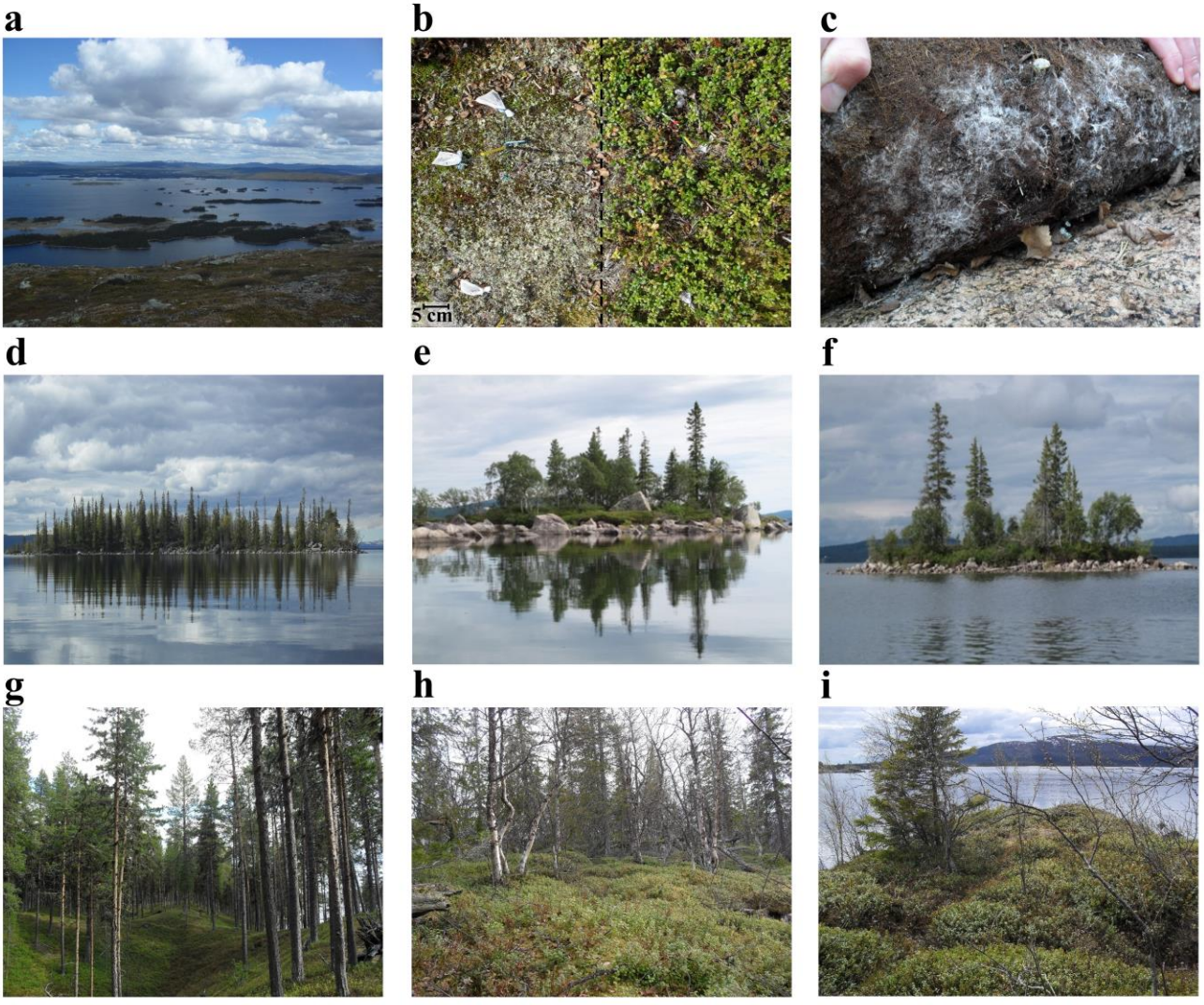

Supplementary Fig. 2 | The relationship between plant diversity and ecosystem multifunctionality for (**a**) the species removal experiment, and (**b**) the functional group removal experiment. Each point represents a separate experimental plot. Bands around the regression lines represent the 95% confidence level intervals. Results of the models testing for effects of island size class (IS) and plant diversity (PD) are given in the lower right corners. Island size classes are represented by colors: large = red, blue = medium, green = small. The results showed that multifunctionality increased with increasing plant diversity and confirm the general model (Supplementary Table 5) in finding that the effects of plant removals did not interact with island size classes.

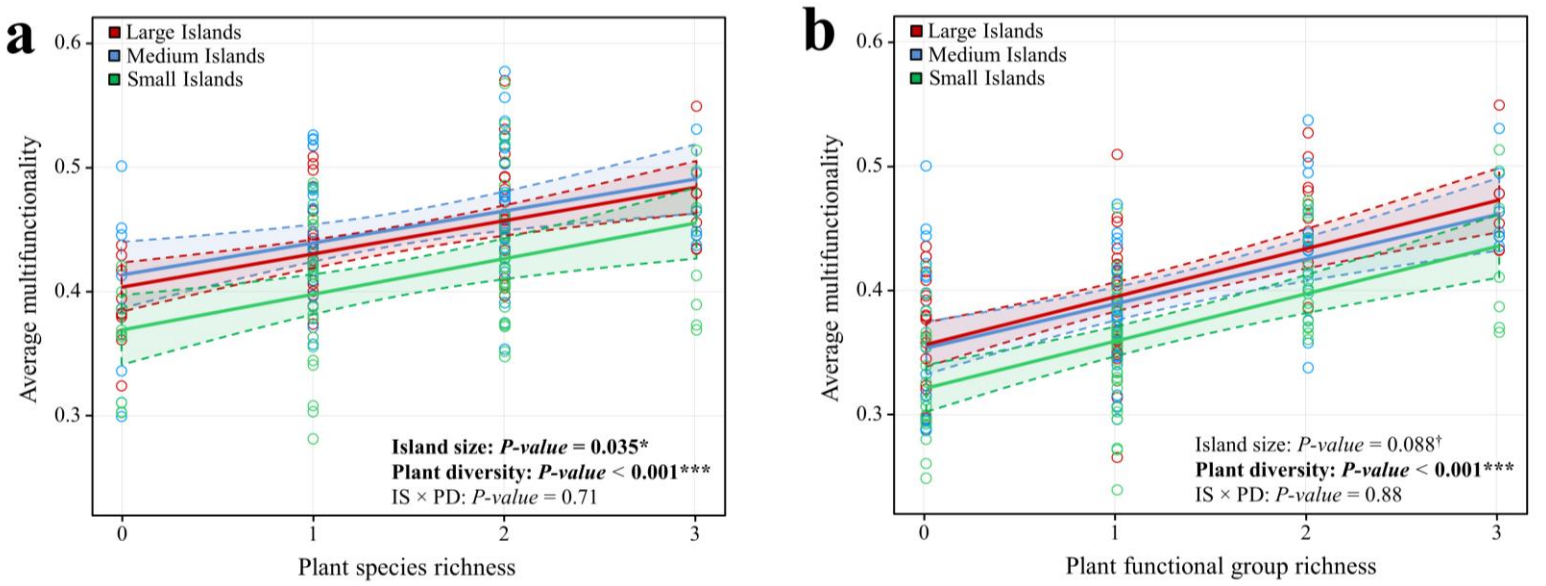

Supplementary Fig. 3 | Sensitivity analysis testing for the robustness of calculated effects of biodiversity loss on ecosystem multifunctionality to the loss of each of the 30 islands (10 each in the large, medium and small size classes) in the species removal experiment (**a**), and functional group removal experiment (**b**). Each point (± 95% confidence intervals) corresponds to the regression coefficient of the plant richness effect extracted from a generalized linear mixed models run on the reduced dataset missing a given island (indicated on the y-axis) at thresholds of 20, 40, 60, and 80% of the maximum. All of the model results are then compared to the solid black vertical line that represents the regression coefficient that is derived when the entire dataset is used. In all cases, the 95% confidence intervals incorporated the black vertical line, indicating that no individual island had a disproportionate effect on our results.

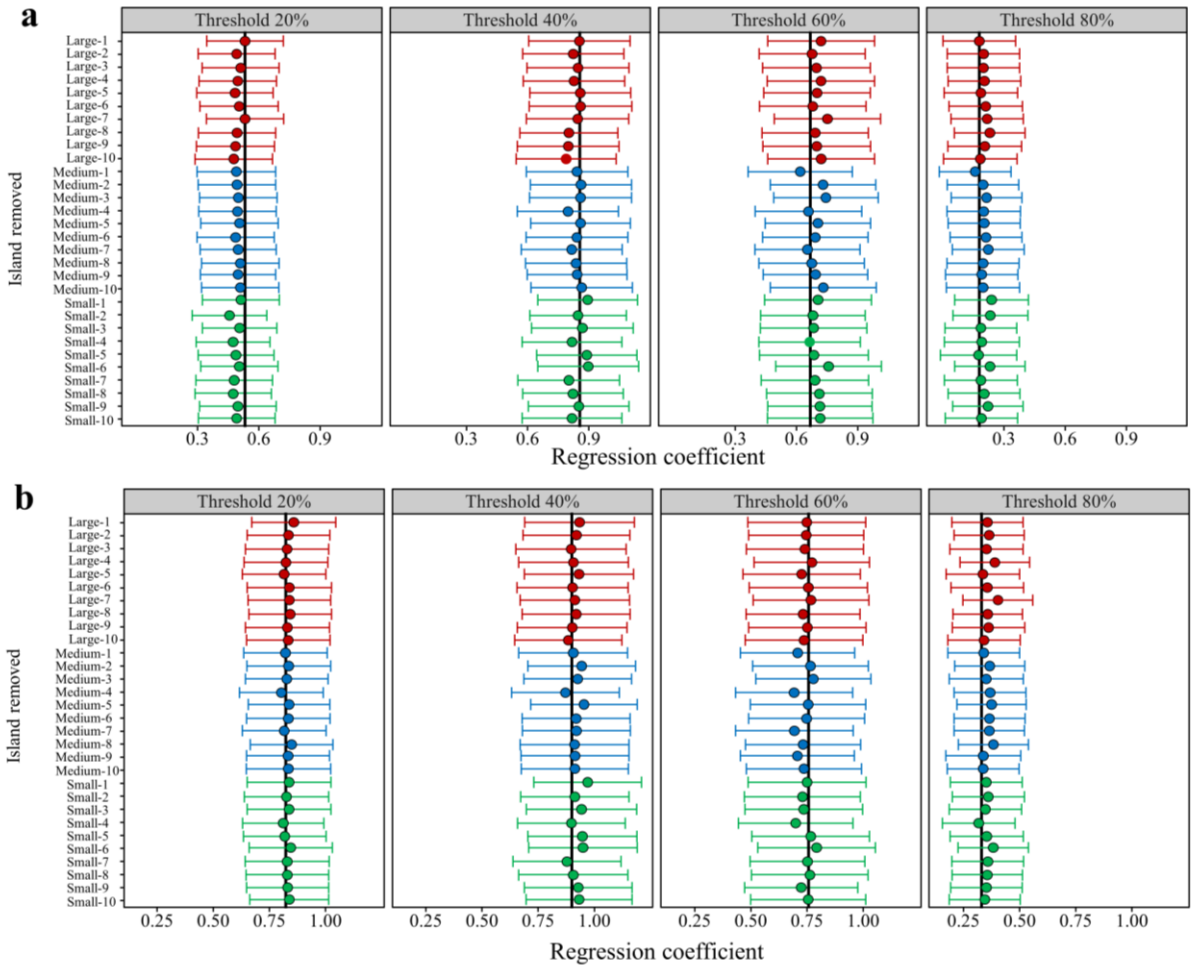

Supplementary Fig. 4 | Slopes between plant diversity and number of functions that reach a defined threshold for a range of thresholds. Lines represent the slope between plant species richness and the number of functions greater than or equal to a threshold value ranging from 5 to 100% of maximum with steps of 1% for each function in the species removal experiment (**a**), and functional group removal experiment (**b**). Island size classes are represented in colors: large = red, blue = medium, green = small. The results show that increasing the number of plant species and functional groups generally increases the number of functions that are above the threshold required for all island size classes.

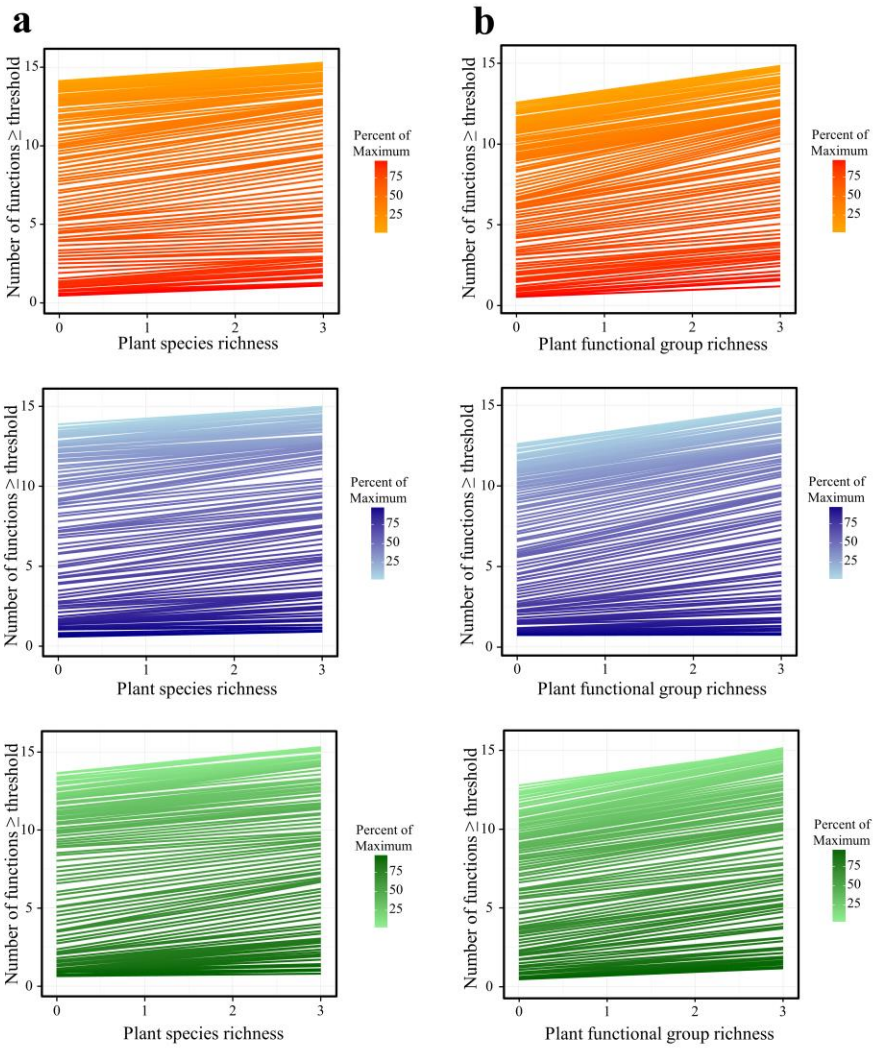

Supplementary Fig. 5 | Effects of plant diversity on ecosystem multifunctionality for a range of thresholds in the species removal experiment (**a**), and functional group removal experiment (**b**). This method evaluates the relationships between plant diversity and the total number of functions that have values that are greater than or equal to a threshold defined as a given percentage of the maximum observed rate of each individual function (ranging from 5 to 100%; see Supplementary Fig. 4 for the range of slopes). Island size classes are represented in colors: large = red, blue = medium, green = small. The dotted curves indicate the changes in the number of functions per unit increment of diversity, with the shaded areas indicating 95% confidence intervals. The threshold of maximum diversity effects (*Tmde*) is the threshold where diversity has its strongest positive or negative effect, and the realized maximum effect of diversity (*Rmde*) is the strength of the relationship (i.e., slope) at the point where diversity has its strongest positive and/or negative effects (i.e., calculated at *Tmde*). The results show that for the plant species removal experiment, *Tmde* peaks at thresholds of about 60% for all island size classes with a *Rmde* of about 1, meaning that about one function is added per addition of one species. For the functional group removal experiment, *Tmde* was relatively similar for large and medium islands but peaked at a lower threshold of 23% in small islands. No significant interactions were found between plant diversity and island size classes at any given threshold.

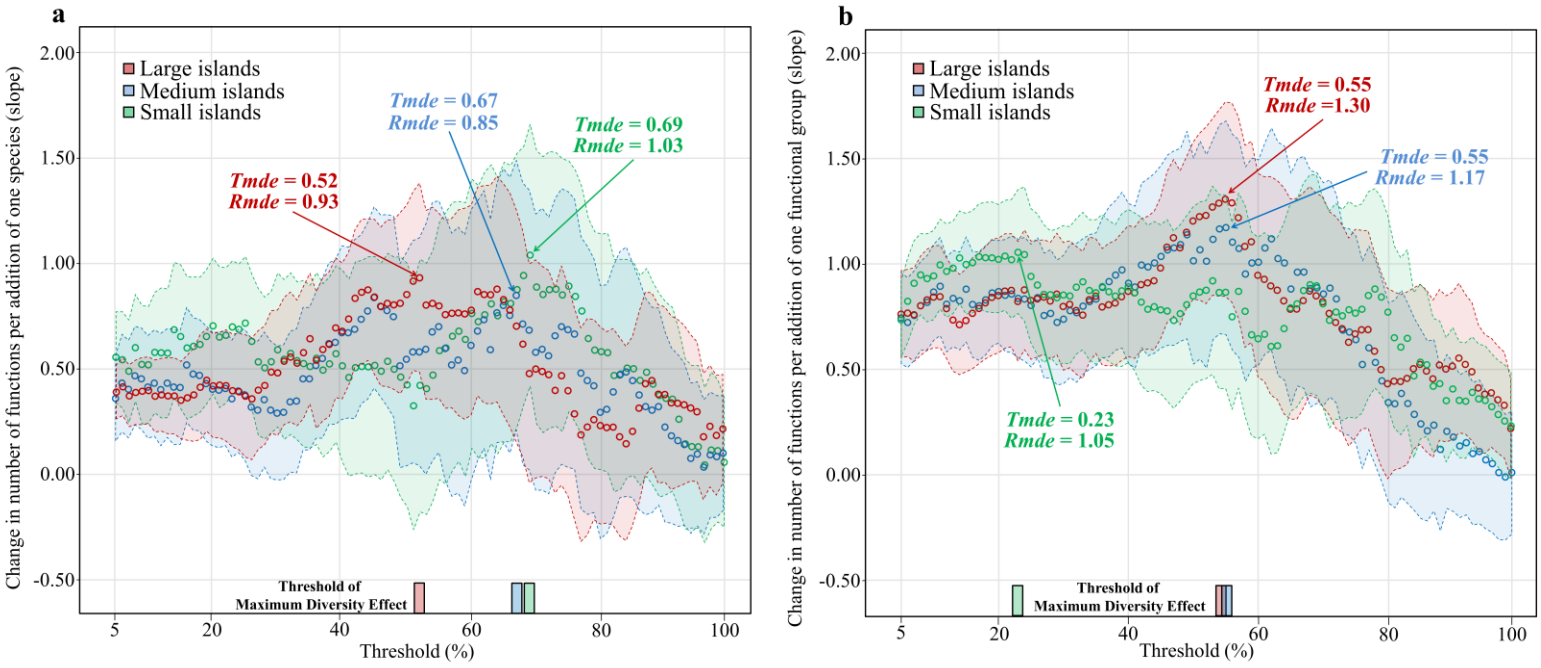

Supplementary Fig. 6 | Additional checks for the species removal experiment analyses depicted in Supplementary Fig. 5, to test for how plant diversity effects on multifunctionality were affected by the selection of functions, for a range of ecosystem multifunctionality thresholds. The number of ecosystem functions was reduced from 15 to 12, 10 and 8 by randomly removing functions to see if the selection of functions affected the result for each island size class (see M&M). For each number of functions, three different examples are shown. The dotted curves indicate the changes in number of functions per unit increment of diversity, with the shaded areas indicating 95% confidence intervals. The results show that overall the effects of plant species richness on the multifunctionality (and the general trends) were maintained regardless of the number of functions selected. Similar results were found for the effects of plant functional group diversity in the functional group removal experiment (results not shown).

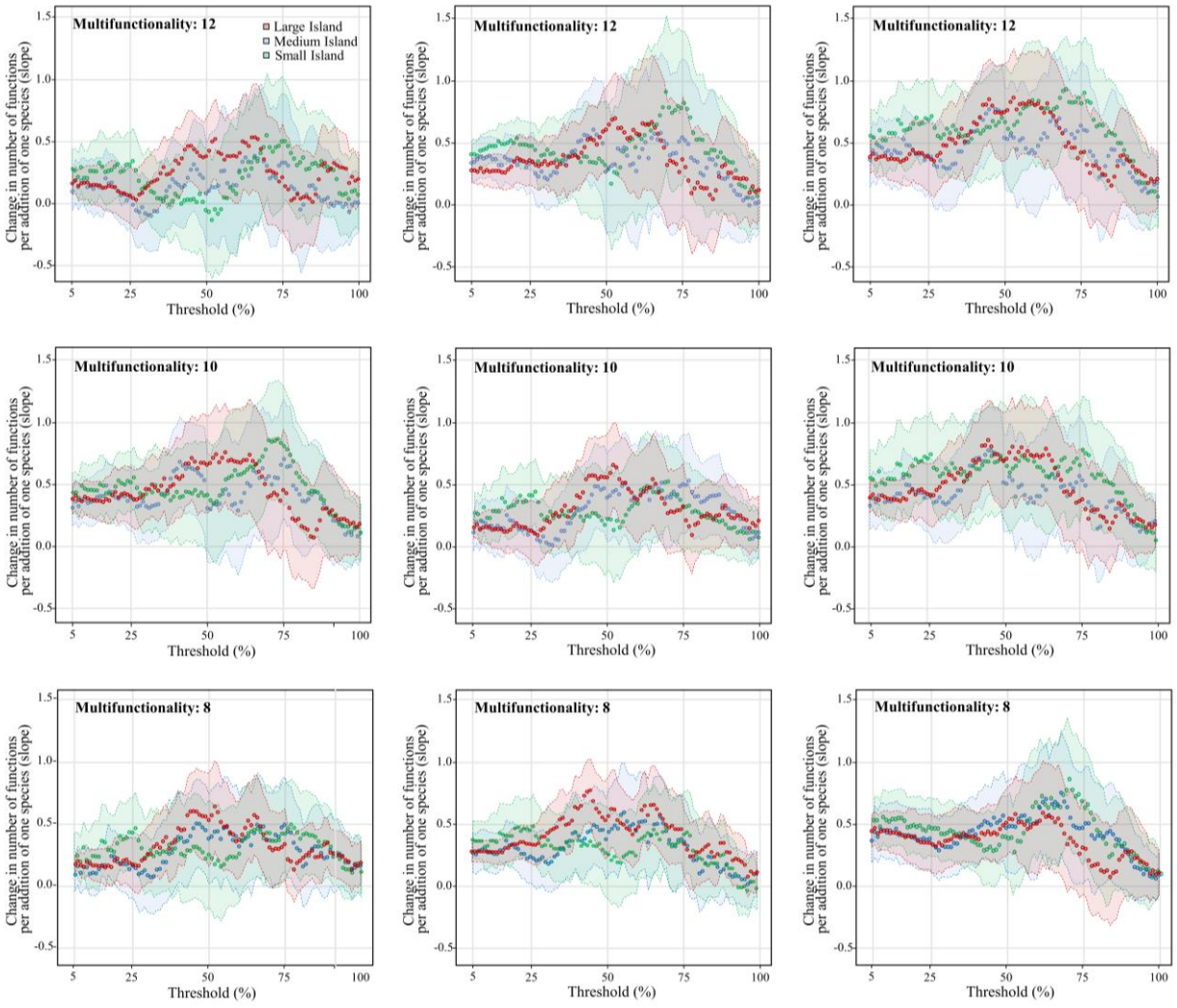

Supplementary Fig. 7 | Non-metric multidimensional scaling (NMDS) ordination based on Bray-Curtis distances of relative abundances of fungal OTUs, for large, medium and small islands. Ordinations were performed to visualize changes in the fungal community structure after (**a**) the removal of the most dominant shrub species present on each island size class (*Vaccinium myrtillus*, *Vaccinium vitis-idaea* and *Empetrum hermaphroditum* on large, medium and small islands respectively), or (**b**) removal of all shrubs. The ellipses represent the average projection area of the experimental plots from the centroid: black *vs* color = absence *vs* presence of the dominant shrub species. The individual lines originating from the center correspond to the distance between the calculated centroid and each of the experimental plots. We also performed vector fitting of the relative proportion of each putative fungal functional group (shown in the top right corner of each panel) using permutation tests (n = 999). ERI = Ericoid mycorrhizal fungi, ECM = Ectomycorrhizal fungi, ROOT = Roots associated mycorrhizal fungi, MOLD = Mold and yeast, SAP = Saprotroph, PATHO = Pathogen and parasite, LICHEN = Lichen, UNK = Unknown.

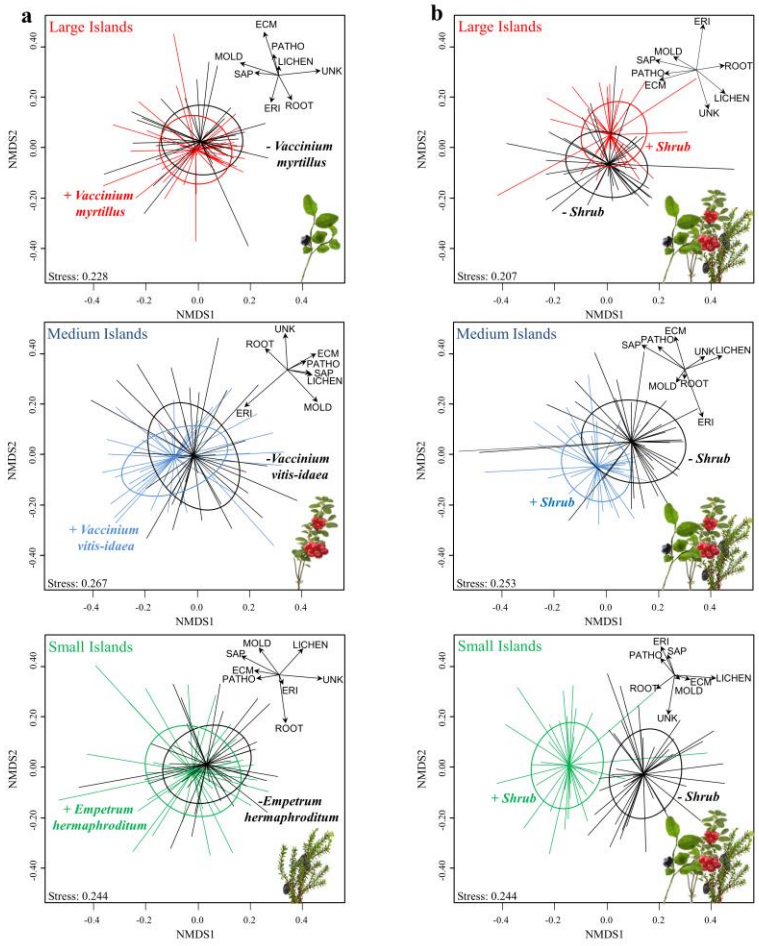

Supplementary Fig. 8 | Boxplots of estimated species richness (α-diversity) (**a**), total fungal relative biomass (**b**) and the fungal to bacterial ratio (**C**) in response to the presence (+S) or absence (-S) of shrubs in each island size class (i.e., large, medium and small). Boxes represent the lower quartile (Q1), median (Q2), upper quartile (Q3) and the interquartile range (IQR = Q3–Q1), which covers the central 50% of the data; whiskers represent 95% of the data. Dark circles within each boxplot represent the mean value. Results from full factorial mixed linear models to test for the effects of plant functional group removals, island size class and their interactions are shown in Table S7.

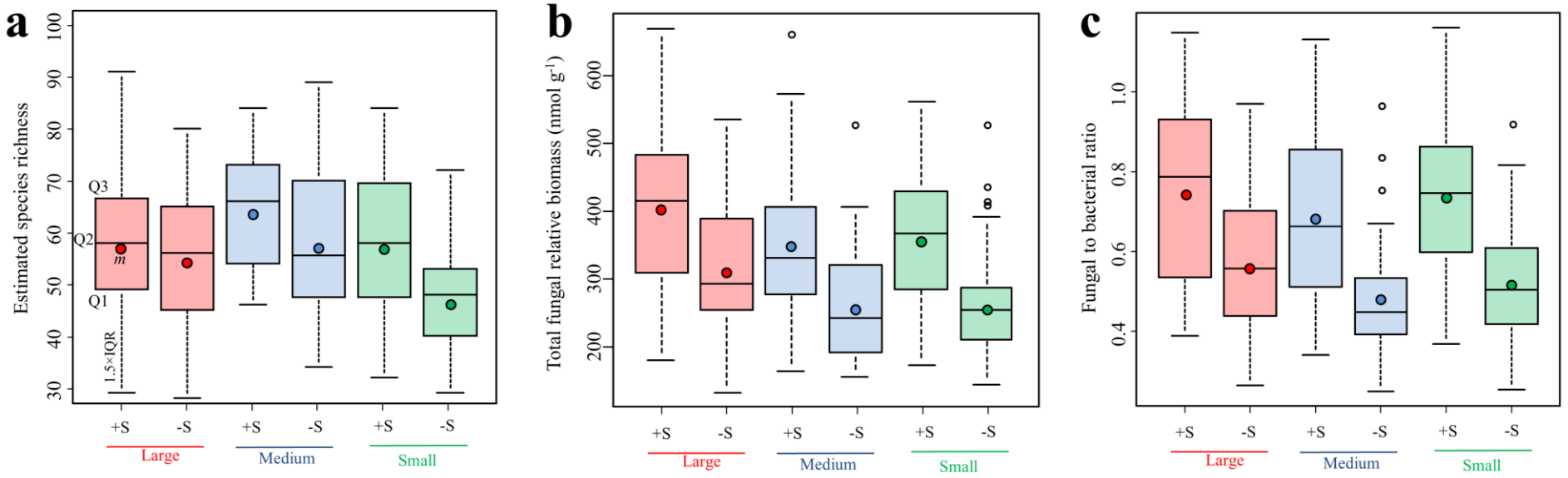

Supplementary Fig. 9 | Shrub removal effects on OTUs in each island size class. Each point represents a separate OTU. The horizontal axis represents the mean abundance of OTUs across all samples and their position along the vertical axis represents the log-fold change in abundance when shrubs are removed relative to when they are present. Enrichment and depletion of OTUs are represented in green and red, respectively. The largest negative effects were found for the small islands with a depletion of 56 OTUs compared to 22 for medium islands 16 OTUs for large islands.

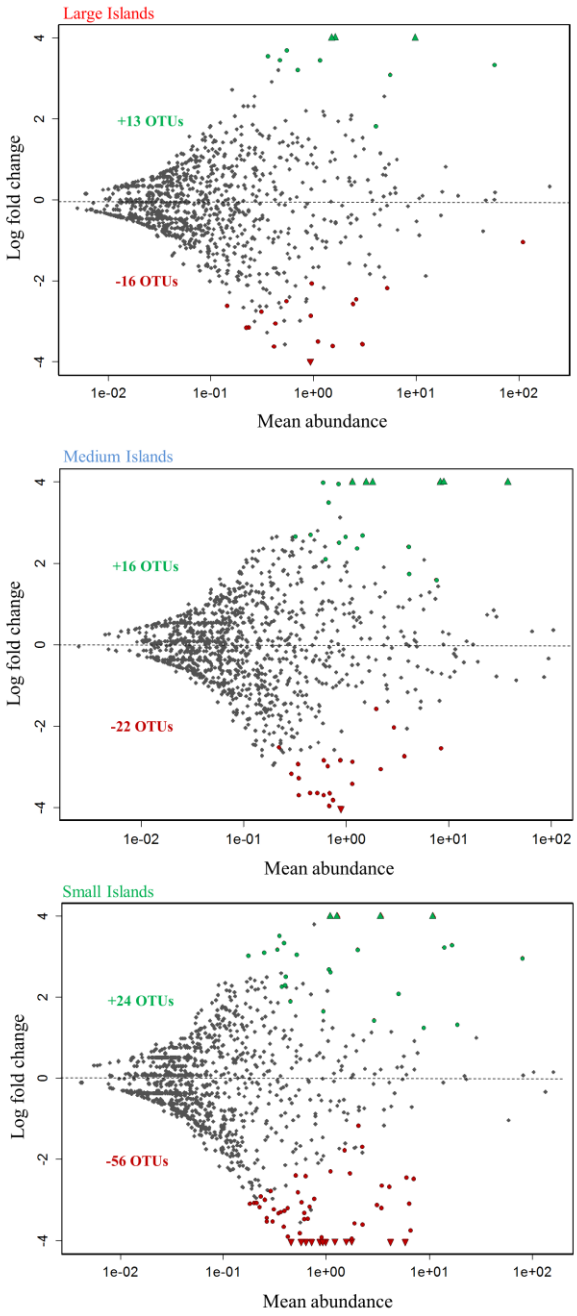

Supplementary Fig. 10 | The relationship between fungal species richness and ecosystem multifunctionality. Relationships are shown between fungal species richness and residuals of the model between multifunctionality and plant diversity plus environmental factors (see Supplementary Tables 9 and 10) for (**a**) the species removal experiment, and (**b**) the functional group removal experiment. Each point represents a separate experimental plot. The dotted curves indicate the changes in number of functions per unit increment of diversity, with the shaded areas indicating 95% confidence intervals. Results of the models testing for the effects of island size class and fungal diversity are given in the lower right corner. Island size classes are represented in colors: large = red, blue = medium, green = small. IS = island size; PD = plant diversity. The results show that even when considering the effects of plant diversity and environmental variables (compare with Fig. 4), fungal diversity impacted multifunctionality for all island size classes.

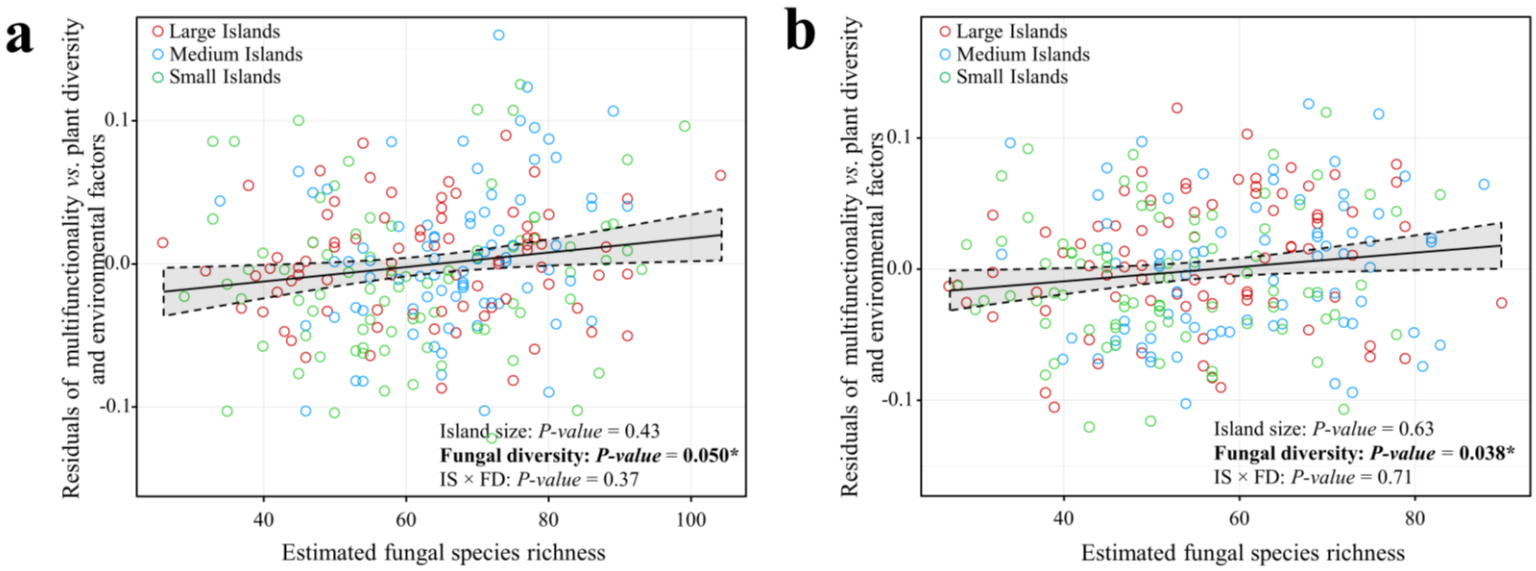

Supplementary Fig. 11 | Slopes between fungal diversity and the number of functions that reach a defined threshold, for a range of thresholds. Lines represent the slopes between fungal species richness and the number of functions greater than or equal to a threshold value ranging from 5 to 100% of maximum with steps of 1% for each function, in the species removal experiment (**a**) and the functional group removal experiment (**b**). Island size classes are represented in colors: large = red, blue = medium, green = small. The results show that increasing the number of fungal species generally increases the number of functions that are above the threshold required for all island size classes, except at high thresholds for medium islands for the functional group removal experiment.

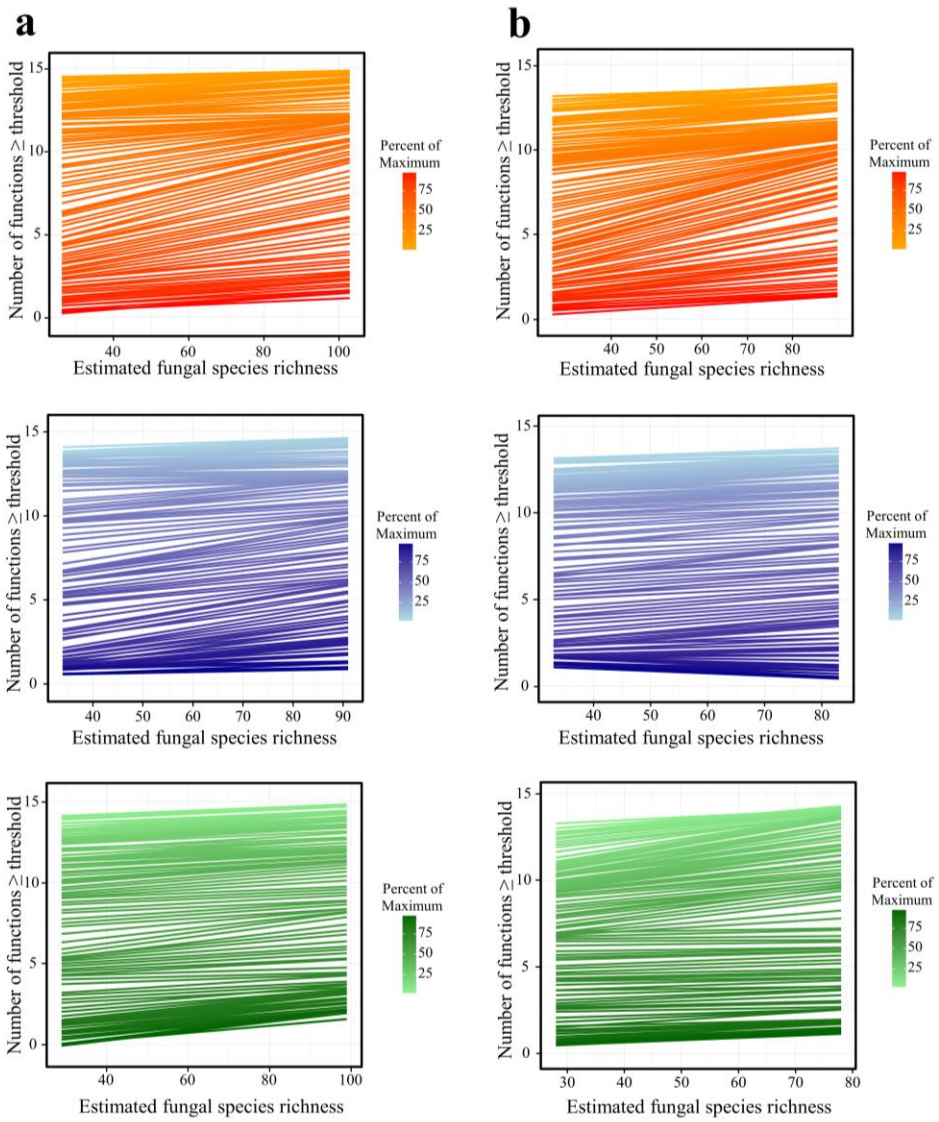

Supplementary Fig. 12 | Effects of fungal diversity on ecosystem multifunctionality for a range of thresholds in the species removal experiment (**a**) and functional group removal experiment (**b**). This method evaluates the relationships between fungal diversity and the total number of functions that have values that are greater than or equal to a threshold defined as a given percentage of the maximum observed rate of each individual function (from 5 to 100%; see Supplementary Fig. S11 for the range of slopes). Island size classes are represented in colors: large = red, blue = medium, green = small. The dotted curves indicate the changes in number of functions per unit increment of diversity, with the shaded areas indicating 95% confidence intervals. The threshold of maximum diversity effects (*Tmde*) is the threshold where diversity has its strongest positive or negative effect, and the realized maximum effect of diversity (*Rmde*) is the strength of the relationship (i.e., slope) at the point where diversity has its strongest positive and/or negative effects (i.e., calculated at *Tmde*). The results show that for the plant species removal experiment, *Tmde* peaks at thresholds of about 60% for all island size classes with a *Rmde* of about 0.050, meaning that about one function is added per addition of 20 fungal species. For the functional group removal experiment, *Tmde* was relatively similar for large and medium islands but peaked at a lower threshold of 21% in small islands. No significant interactions were found between plant diversity and island size classes except for thresholds of over 85%.

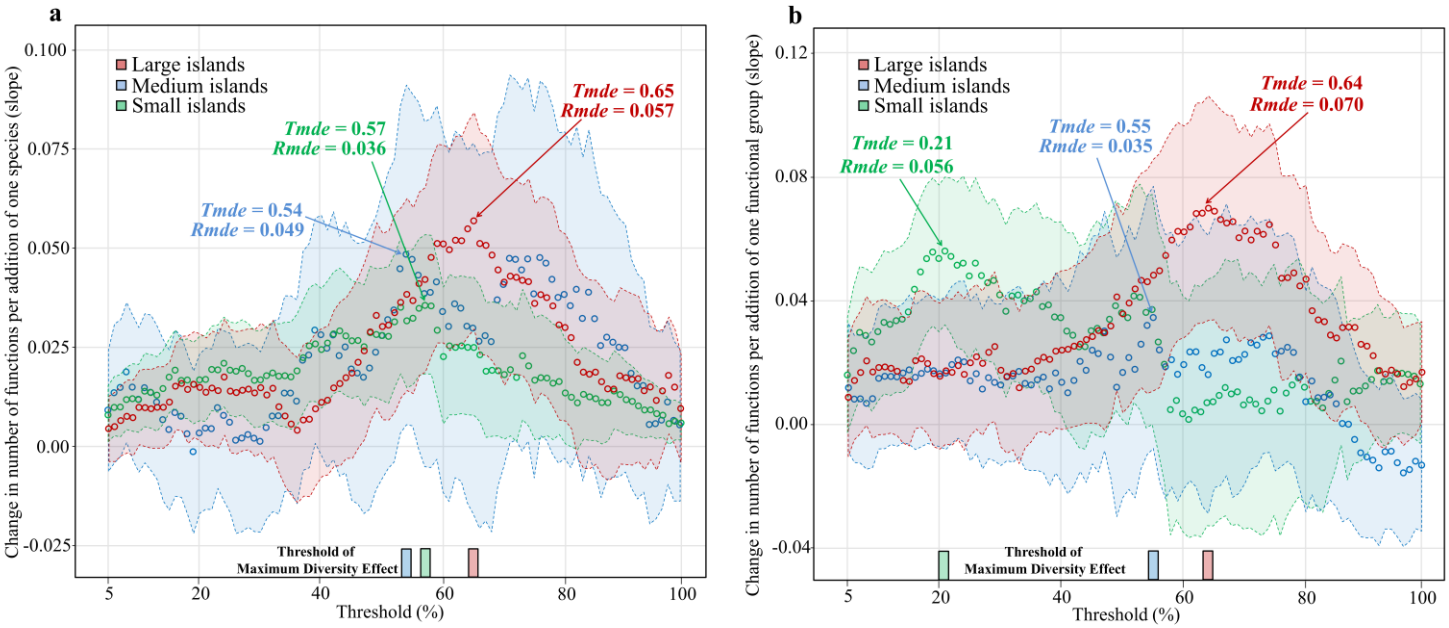

Supplementary Fig. 13 | Additional checks for the functional group removal experiment analyses depicted in Supplementary Fig. 12, to test for how fungal diversity effects on multifunctionality were affected by the selection of functions, for a range of ecosystem multifunctionality thresholds. The number of ecosystem functions was reduced from 15 to 12, 10 and 8 by randomly removing functions to see if the selection of functions affected the result for each island size class (see M&M). For each number of functions, three different examples are shown. The dotted curves indicate the changes in number of functions per unit increment of diversity with the shaded areas indicating 95% confidence intervals. The results show that overall the effects of fungal species richness on the multifunctionality (and the general trends) were maintained regardless of the number of functions selected. Similar results were found for the effects of fungal diversity in the species removal experiment (results not shown).

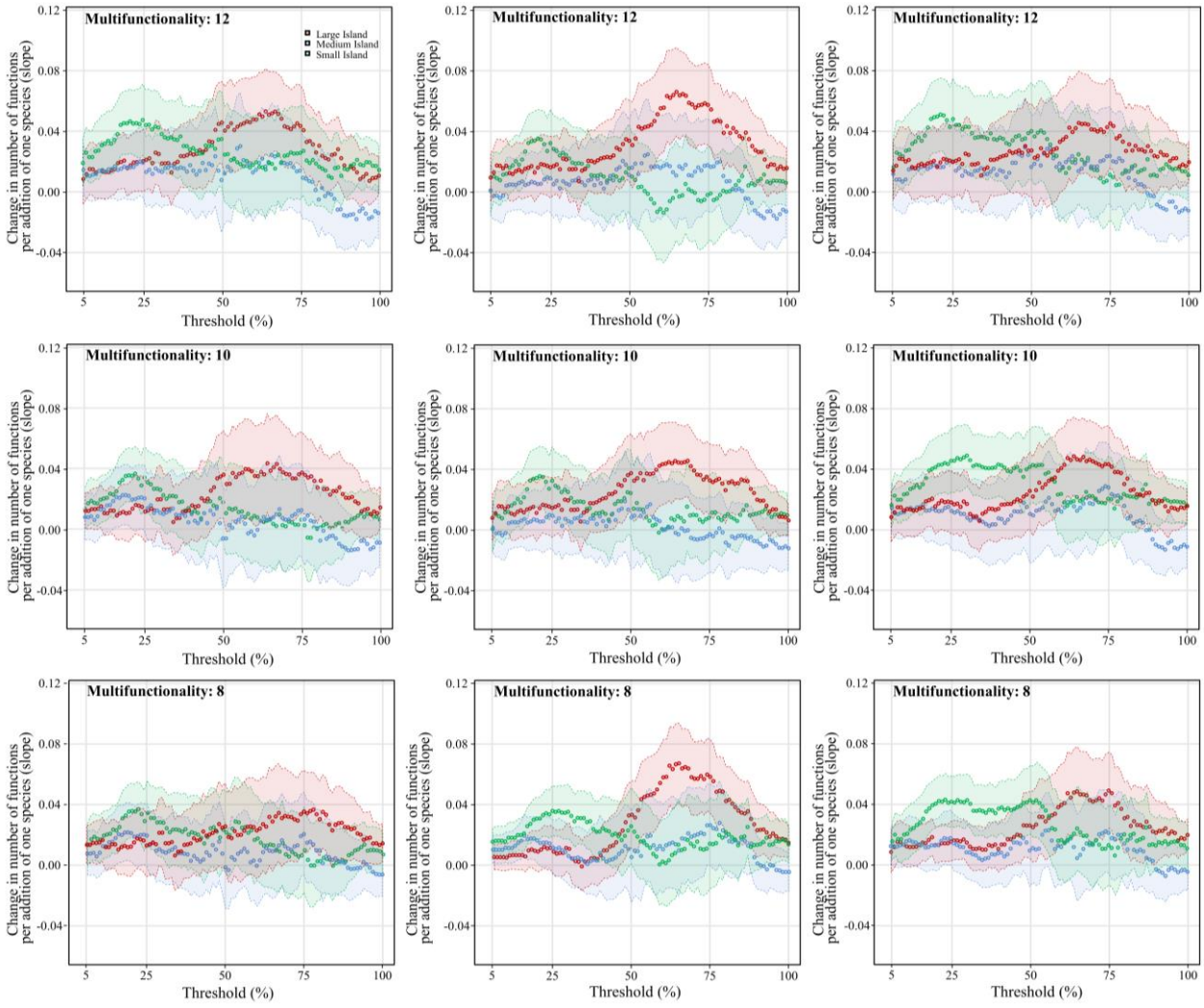

References in Supplementary Information

1 Ihrmark, K. *et al.* New primers to amplify the fungal ITS2 region–evaluation by 454-sequencing of artificial and natural communities. *FEMS Microbiology Ecology* **82**, 666-677 (2012).

2 Clemmensen, K. E., Ihrmark, K., Durling, M. B. & Lindahl, B. D. in *Microbial Environmental Genomics (MEG)* (eds F Martin & S Uroz) 61-88 (Springer, 2016).

3 White, T. J., Bruns, T., Lee, S. & Taylor, J. W. in *PCR protocols: a guide to methods and applications* Vol. 18 (eds M A Innis, D H Gelfand, J Sninsky, & T J White) 315-322 (Academic Press, 1990).

4 Kõljalg, U. *et al.* Towards a unified paradigm for sequence-based identification of fungi. *Molecular Ecology* **22**, 5271-5277 (2013).

5 Tedersoo, L. *et al.* Global diversity and geography of soil fungi. *Science* **346**, 1256688 (2014).

6 Wardle, D. A., Hörnberg, G., Zackrisson, O., Kalela-Brundin, M. & Coomes, D. A. Long-term effects of wildfire on ecosystem properties across an island area gradient. *Science* **300**, 972-975 (2003).

7 Lagerström, A., Nilsson, M. C., Zackrisson, O. & Wardle, D. Ecosystem input of nitrogen through biological fixation in feather mosses during ecosystem retrogression. *Functional Ecology* **21**, 1027-1033 (2007).

8 DeLuca, T., Nilsson, M.-C. & Zackrisson, O. Nitrogen mineralization and phenol accumulation along a fire chronosequence in northern Sweden. *Oecologia* **133**, 206-214 (2002).

9 Gundale, M. J., From, F., Bach, L. H. & Nordin, A. Anthropogenic nitrogen deposition in boreal forests has a minor impact on the global carbon cycle. *Global Change Biology* **20**, 276-286 (2014).

10 Anderson, J. & Domsch, K. A physiological method for the quantitative measurement of microbial biomass in soils. *Soil Biology and Biochemistry* **10**, 215-221 (1978).

11 Gundale, M. J., Fajardo, A., Lucas, R. W., Nilsson, M. C. & Wardle, D. A. Resource heterogeneity does not explain the diversity–productivity relationship across a boreal island fertility gradient. *Ecography* **34**, 887-896 (2011).

12 Baldock, J. *et al.* Quantifying the allocation of soil organic carbon to biologically significant fractions. *Soil Research* **51**, 561-576 (2014).

13 Baldock, J., Masiello, C., Gelinas, Y. & Hedges, J. Cycling and composition of organic matter in terrestrial and marine ecosystems. *Marine Chemistry* **92**, 39-64 (2004).

14 Baldock, J., Hawke, B., Sanderman, J. & Macdonald, L. Predicting contents of carbon and its component fractions in Australian soils from diffuse reflectance mid-infrared spectra. *Soil Research* **51**, 577-595 (2014).

15 Baldock, J. *et al.* Aspects of the chemical structure of soil organic materials as revealed by solid-state 13 C NMR spectroscopy. *Biogeochemistry* **16**, 1-42 (1992).

16 Baldock, J. A. & Smernik, R. J. Chemical composition and bioavailability of thermally altered Pinus resinosa (Red pine) wood. *Organic Geochemistry* **33**, 1093-1109 (2002).

17 Frostegård, Å., Tunlid, A. & Bååth, E. Phospholipid fatty acid composition, biomass, and activity of microbial communities from two soil types experimentally exposed to different heavy metals. *Applied and Environmental Microbiology* **59**, 3605-3617 (1993).

18 Blagodatskaya, E. & Kuzyakov, Y. Active microorganisms in soil: critical review of estimation criteria and approaches. *Soil Biology and Biochemistry* **67**, 192-211 (2013).
19 Denef, K., Roobroeck, D., Wadu, M. C. M., Lootens, P. & Boeckx, P. Microbial community composition and rhizodeposit-carbon assimilation in differently managed temperate grassland soils. *Soil Biology and Biochemistry* **41**, 144-153 (2009).
20 Zelles, L. Fatty acid patterns of phospholipids and lipopolysaccharides in the characterisation of microbial communities in soil: a review. *Biology and Fertility of Soils* **29**, 111-129 (1999).
21 Bligh, E. G. & Dyer, W. J. A rapid method of total lipid extraction and purification. *Canadian Journal of Biochemistry and Physiology* **37**, 911-917 (1959).
22 White, D., Davis, W., Nickels, J., King, J. & Bobbie, R. Determination of the sedimentary microbial biomass by extractible lipid phosphate. *Oecologia* **40**, 51-62 (1979).
23 Frostegård, Å. & Bååth, E. The use of phospholipid fatty acid analysis to estimate bacterial and fungal biomass in soil. *Biology and Fertility of Soils* **22**, 59-65 (1996).
24 Wardle, D. A., Zackrisson, O., Hörnberg, G. & Gallet, C. The influence of island area on ecosystem properties. *Science* **277**, 1296-1299 (1997).
25 Dıaz, S., Symstad, A. J., Chapin, F. S., Wardle, D. A. & Huenneke, L. F. Functional diversity revealed by removal experiments. *Trends in Ecology & Evolution* **18**, 140-146 (2003).
26 Wardle, D. A. *et al.* Ecological linkages between aboveground and belowground biota. *Science* **304**, 1629-1633 (2004).
27 Wardle, D. A. *et al.* Linking vegetation change, carbon sequestration and biodiversity: insights from island ecosystems in a long-term natural experiment. *Journal of Ecology* **100**, 16-30 (2012).
28 Clemmensen, K. *et al.* Roots and associated fungi drive long-term carbon sequestration in boreal forest. *Science* **339**, 1615-1618 (2013).
29 Galloway, J. N. *et al.* Nitrogen cycles: past, present, and future. *Biogeochemistry* **70**, 153-226 (2004).
30 Chapin III, F. S., Matson, P. A. & Vitousek, P. *Principles of terrestrial ecosystem ecology*. (Springer, 2011).
31 Aerts, R. & Chapin, F. S. The mineral nutrition of wild plants revisited: a re-evaluation of processes and patterns. *Advances in Ecological Research* **30**, 1-67 (1999).
32 Geisseler, D., Horwath, W. R., Joergensen, R. G. & Ludwig, B. Pathways of nitrogen utilization by soil microorganisms–a review. *Soil Biology and Biochemistry* **42**, 2058-2067 (2010).
33 Filippelli, G. M. The global phosphorus cycle: past, present, and future. *Elements* **4**, 89-95 (2008).
34 Vitousek, P. M., Porder, S., Houlton, B. Z. & Chadwick, O. A. Terrestrial phosphorus limitation: mechanisms, implications, and nitrogen–phosphorus interactions. *Ecological applications* **20**, 5-15 (2010).
35 Peñuelas, J. *et al.* Human-induced nitrogen–phosphorus imbalances alter natural and managed ecosystems across the globe. *Nature Communications* **4** (2013).
36 Cross, A. F. & Schlesinger, W. H. A literature review and evaluation of the. Hedley fractionation: Applications to the biogeochemical cycle of soil phosphorus in natural ecosystems. *Geoderma* **64**, 197-214 (1995).
37 Holford, I. Soil phosphorus: its measurement, and its uptake by plants. *Soil Research* **35**, 227-240 (1997).

38 Cleveland, C. C., Townsend, A. R. & Schmidt, S. K. Phosphorus limitation of microbial processes in moist tropical forests: evidence from short-term laboratory incubations and field studies. *Ecosystems* **5**, 0680-0691 (2002).
39 Gundale, M. J., Nilsson, M. C., Pluchon, N. & Wardle, D. A. The effect of biochar management on soil and plant community properties in a boreal forest. *GCB Bioenergy* (2015).
40 Lal, R. Soil carbon sequestration impacts on global climate change and food security. *Science* **304**, 1623-1627 (2004).
41 Lal, R. Forest soils and carbon sequestration. *Forest Ecology and Management* **220**, 242-258 (2005).
42 Bardgett, R. D., Freeman, C. & Ostle, N. J. Microbial contributions to climate change through carbon cycle feedbacks. *ISME* **2**, 805-814 (2008).
43 Bardgett, R. D. & Wardle, D. A. *Aboveground-belowground linkages: biotic interactions, ecosystem processes, and global change*. (Oxford University Press, 2010).
44 Nilsson, M.-C. & Wardle, D. A. Understory vegetation as a forest ecosystem driver: evidence from the northern Swedish boreal forest. *Frontiers in Ecology and the Environment* **3**, 421-428 (2005).
45 Nannipieri, P. *et al.* Microbial diversity and soil functions. *European Journal of Soil Science* **54**, 655-670 (2003).
46 Lussenhop, J. Mechanisms of microarthropod-microbial interactions in soil. *Advances in Ecological Research* **23**, 1-33 (1992).
47 A'Bear, A. D., Jones, T. H. & Boddy, L. Size matters: What have we learnt from microcosm studies of decomposer fungus–invertebrate interactions? *Soil Biology and Biochemistry* **78**, 274-283 (2014).
48 Trap, J., Bonkowski, M., Plassard, C., Villenave, C. & Blanchart, E. Ecological importance of soil bacterivores for ecosystem functions. *Plant and Soil* **398**, 1-24 (2016).
49 Mori, A. S. *et al.* Low multifunctional redundancy of soil fungal diversity at multiple scales. *Ecology Letters* **19**, 249-259 (2016).